DOE/PC/70768--T2

DE92 000283

TECHNICAL PROGRESS REPORT

KINETICS OF COAL PYROLYSIS AND DEVOLATILIZATION

For the period February 1, 1987 - April 30, 1987

Work Performed under Contract No. DE-AC22-84PC70768

For

U. S. Department of Energy
Pittsburgh Energy Technology Center
P. O. Box 10940
Pittsburgh, PA 15236

By

United Technologies Research Center
East Hartford, CT 06108

DISCLAIMER

SUMMARY

An experimentally based, conceptual model of the devolatilizaiton of a HV bituminous coal is outlined in this report. This model contends that the relative dominance of a process type-chemical kinetic, heat transport, mass transport -- varies with the extent of reaction for a given set of heating conditions and coal type and with experimental conditions for a given coal type and extent of reaction. The relevant "reference" conditions of interest for direct utilization are rapid transient heating of small (< 100 micron) particles to temperatures of 1000°C or greater. The onset of devolatilization is signaled by the rapid evolution of tars during the particle temperature rise from 300 to 600°C. It appears the rate of particle mass loss during this phase of devolatilization is primarily controlled by heat transfer from the environment to the particle. Mass transfer and chemical kinetics determine the particle mass loss rate during the next stage (600-800°C), while the residual char degassing is primarily controlled by chemical kinetic phenomena. Thus the rate of the devolatilization mass loss process is dominated initially by heat transfer processes, then coupled mass transfer and chemical kinetics, and finally by chemical processes alone. However, the chemical composition of the initial tars are determined primarily by the chemical characteristics of the parent coal. Chemically controlled gas phase reactions of the initial tars and coupled mass transfer and chemically controlled reactions of heavy tars determine the bulk of the light gas yields. For a HV bituminous coal this conceptual model serves to quantify the "Two-Component Hypothesis" of volatiles evolution.

The model postulatew that the overall rates of coal devolatilization should vary with coal type insofar as the characteristics of the parent coal determine the potential tar yield and the chemical characteristics of the initial tars. Experimental evidence indicates chemical characteristics and yields of "primary" tars vary significantly with coal type. Consequently, the conceptual model would indicate a shift from transport to chemical dominance of rate processes with variation in coal type. Using the conceptual model, UTRC has been able to correlate initial mass loss with a heat transfer index for a wide range of conditions for high tar yielding coals.

Introduction

An examination of the literature (1) indicates "models" of coal devolatilization and pyrolysis are successful in describing data generated in specific heating conditions only. Extrapolation of kinetic models developed to describe a particular experimental configuration to other heating conditions has not been successful. Many factors contribute to the "apparent" discrepancies and inconsistencies noted among various experiments (1, 2), and even among the investigations performed by a single investigator (3, 4, 5, 6). Among these are: the inherent complexity and ill-defined physical and chemical nature of coal itself; the irreversible, transient nature of coal devolatilization; the lack of a common sample set in the various coal devolatilization studies; the failure of many models to explicitly define the basic assumptions employed in their modeling efforts and thereby provide a basis of model comparison; the lack of formulation of the aspect of coal devolatilization of primary concern in the model description.

It is known, for example, that the devolatilization of a high volatile bituminous coal is dominated, on a mass loss basis, by the evolution of heavy hydrocarbon species. The mass loss of a subbituminous coal in the same conditions may consist of equal mass fractions of heavy hydrocarbons (tars) and light gases. A lignite sample devolatilizing in the same heating conditions may consist mainly of light gases. In addition, resultant char particle morphologies vary significantly with coal type. "Weight" loss kinetic model comparisons of these three coals can only be made if the assumptions employed with respect to coal structure, devolatilization product source terms in the kinetic model, and the effect of changing product

distribution and char morphology on the transient particle temperature history are explicitly stated.

It is obvious from the brief description above that an engineering kinetics model will only be as valid and generally applicable as the fundamental understanding that serves as its basis. Unless a correct phenomenological description of coal devolatilization can be formulated on the basis of an accurate understanding of coal structure and behavior, an empirical, engineering description of coal devolatilization is not possible. "Engineering" herein means less chemical detail regarding product composition and structure, not less accuracy with respect to the rates of particle mass loss.

The significance of development of a fundamental understanding of coal devolatilization and accurate descriptions of the rates of coal devolatilization requires an understanding of the coal combustion process. Figure 1 shows the coal combustion sequence, indicating coal itself does not burn, but rather rapidly devolatilizes. The resultant volatiles and char species burn. The volatiles combustion process contributes to the near burner flame stability peak flame temperatures, and is directly responsible for major fractions of the flame sooting tendency, and fuel related NO_x formation. The devolatilization process and volatiles burnout process are indirectly responsible for char burnout times by determining aerodynamic and reactivity properties of the resultant char particles, that is, particle

swelling, porosity, density, active surface area, carbon mass.

Approach

Due to the nature of coal structure, any coal devolatilization process involves coupled chemical kinetics, heat transfer and mass transfer phenomena. As a result, no single coal devolatilization experiment and accompanying analysis will result in a model of coal devolatilization that can be extrapolated to a different set of heating conditions for a given coal, or a different coal within a given set of heating conditions. It is even doubtful that a single laboratory can cover the range of experimental conditions desired while establishing the modeling effort required to develop a comprehensive model. Consequently, this investigation utilizes a multi-reactor, multi-laboratory, multi-investigator approach to establish an understanding of coal devolatilization and to develop the fundamental and engineering kinetic models which follow.

The laboratory and modeling efforts are performed using DOE provided samples (PSOCXXXX-D) from a range of major coal seams. The entire range of major coal provinces is spanned by the sample set, as is the range of coal ranks. Figure 2 displays the location, on a pseudo-coalification band plot of the ten "core" sample types provided by DOE-PETC. These samples and the particle sizes of the same samples are being used by all laboratories engaged in this investigation as well as laboratories performing related studies, such

as Sandia Laboratories, DOE-METC, UNDERC, etc.

Reactor Systems

Within this investigation, a range of heating conditions is employed in formulating a general phenomenological model of coal devolatilization and a set of model premises. Historically, a range of heating conditions has been employed to deconvolute the phases of coal devolatilization, while at the same time generating and capturing enough of the devolatilization product types evolved in each phase to allow subsequent analyses. Figure 3 displays the range of transient heat fluxes used to heat different sized particles and notes the type of heating environment usually associated with each heating condition. In this investigation United Technologies Research Center (UTRC) has established a heated grid (HG), flash lamp (FL), and an entrained flow (EF) devolatilization system. Pennsylvania State University (PSU) utilizes a hot wall and hot gas entrained flow (PSU-EF) system.

UTRC's entrained flow reactor differs from the PSU-EF in that the gases are not preheated, that is, the peak gas temperature is several hundred degrees lower than the wall temperature in order to minimize secondary reactions of evolved tars. These experiments cover a wide range of heat transfer rates, from several tenths watts/cm^2 (UTRC-HG) to several hundred watts/cm^2 (UTRC-FL), generate different thermal environments for the evolved volatiles, and vary widely in the component mode of heat transfer to the

devolatilizing particles.

In vacuum conditions, the UTRC-HG transfers heat to the particles mainly via radiation, while in one atmosphere of helium gas phase, conduction from the wire mesh to the particles contributes a component comparable in magnitude to the radiation. The UTRC-FL is a purely radiative transfer process. The UTRC-EF heats particles mainly by radiation to equilibrium with the local gas tempeerature. The PSU-EF heat transfer is dominated by gas phase conduction/convection to the particles. In all cases, measurements of the in-situ heat transfer components within the reactor system are either measured directly or determined from measurements of parameters directly related (See Table I).

Figures 4, 5, and 6 display the essential components of the UTRC-EF reactor and product separation system -- the reactor, the aerosol-char separation device, the sample collection system. Figures 7, 8, and 9 display the total power density, the radiative power density component and gas temperature profiles as a function of reactor position. The total and radiative flux rate profiles were measured with specially designed probes.

The UTRC-EF creates a heat transfer field in which entrained particles are heated by radiation to the local, axial, entrained gas temperature within the reactor. Incident, center-line radiative flux rates range from several watts/cm^2 at wall temperatures of 750^{o}C to 25 watts/cm^2 at wall

temperatures of 1270°C. The particles quickly dissipate some of the absorbed energy by convective loss to the entrainment gas. Corresponding net power densities experienced by the particles for various reactor wall temperatures and during the particle temperatures of greatest mass loss, 300-600°C, range from 0.2 watts/cm^2 to 4 watts/cm^2. Estimated particle heating rates are on the order of 5000-7000°C/sec in these conditions, greater than that reproducibly obtainable in the UTRC-HG, but less than that expected in pfc firing conditions.

For the PSOC 1451D coal, the ash-tracer determined volatiles yield for two particle sizes is shown in Figure 10. As indicated, despite the factor of three difference in particle size, the reactor temperature sensitivity of the mass loss is very similar between the size cuts. Transient particle temperature calculations indicate both size cuts should follow nearly the same temperature histories in this reactor, in which the particles are heated by radiation and rapidly equilibriate with the local gas temperature by conduction across a gas-particle boundary layer. Figure 11 shows the relative gas yields, normalized with respect to maximum yields of each gas and plotted with respect to peak reactor gas temperature. Gas phase peak temperatures are used to plot gas yields since it is known that gas phase reactions of evolved tars, so called "secondary" reactions of tars, are responsible for large fractions of the light gas yields observed during coal devolatilization (7,8). It is noted that significant increases in acetylene and hydrogen cyanide are not observed until peak gas temperatures of 700°C

are reached. At lower gas temperatures light gas yields are dominated by CH_4, C_2H_4, CO and H_2O, but these gases account for only 10 - 15 % of the 0.20 - 0.25 mass fraction volatiles yield observed for wall temperatures to 900°C. Tar species dominate the mass loss at the lower reactor wall and gas temperatures corresponding to particle temperatures of 600°C or lower. For HV bituminous coals, appreciable tar yields, 0.10 - 0.15 mass fraction, are observed for wall temperatures of 790°C and peak gas temperatures of 350°C. These tars are hydrogen rich and sulfur and oxygen poor relative to either the parent coal or the average composition of the tars at the conditions of maximum tar yield. Peak tar yields are observed at wall temperature between 930 and 1020 C and peak gas temperature between 510 and 665°C.

The tar evolution process resembles a distillation process insofar as the hydrogen rich components vaporize first (See Table II). Similar behavior is displayed by the 63-75 micron cut of the same coal (See Table III). A distillation-like tar evolution process would also imply that species of lower average molecular weight should be observed in the initial tar yields relative to that observed for total integrated tar species. The data of Table IV indicates that such behavior is indeed observed in conditions in which secondary reactions of tars are minimized (Table IV, UTRC-EF results).

High gas phase reactor temperatures which promote so-called "secondary" gas phase pyrolysis reactions of tars should promote reductions in molecular

weight characteristics of tars, relative to the initial tar species evolved. Tars collected from the PSU-EF reactor, wherein gas and wall temperatures are matched, display such characteristics as a function of both reactor temperature and residence time within the reactor. The "initial" low residence time tars display molecular weight characteristics similar to those collectively evolved in the UTRC-EF reactor to the point of maximum tar yield. However, the exposure to the high gas temperatures in the PSU-EF reactor quickly leads to pyrolytic reductions in the molecular weight characteristics of these initial tars as well as decreases in the hydrogen content. One would also expect increases in the C_2H_2, CO, HCN, C_2H_4 yields, as observed in the highest gas temperature data of the UTRC-EF reactor, as the tars undergo these secondary reactions.

Figure 12 displays the power density dissipation from the surface of the stainless steel wire mesh as a function of screen temperature. As noted, a greater power input to the screen in helium conditions is required to achieve equivalent temperatures reached in low pressure conditions. Screen temperatures are measured by optically isolated chromel-alumel thermocouples spot welded to a screen strand. The essential points to note are: a) the magnitude of the power dissipation from the screen surface ranges from a few tenths of watt/cm^2 at low screen temperatures to several watts/cm^2 at temperatures approaching 1000^{o}C; b) the He gas enhances the heat loss dissipation by providing an alternate loss mechanism; c) the radiative and conductive power dissipation from the screen are the modes of heat transfer to

the enfolded coal particles; d) the net power density to the particles within the folds of the screen at screen temperatures corresponding to the major tar evolution, 400-700°C, is comparable in magnitude to the net power density determined in the UTRC-EF at conditions of maximum tar yield, 1-2 watts/cm^2, although the mix of incident and loss modes varies significantly with reactor type.

Table V displays some typical product yields obtained by heating samples of PSOC 1451D in this manner. Again, heavy hydrocarbons, tars, dominate the measurable volatiles mass loss for devolatilization runs characterized by peak screen temperatures of 400°C to 700°C. Light gas yields of C_2H_2 and HCN, characteristic of high temperature (700°C+) gas phase reactions of tars are notably absent in the yield structure. Such observations indicate the major fraction of the tar species is formed and rapidly transferred through the hot gas-grid-sample complex at temperatures below 700°C. Once through the grid hot zone the species are rapidly quenched by the cool ambient gas or cold reactor walls.

Molecular weight characteristics of a number of UTRC-HG produced tars are shown in Table VI. The number and weight average molecular weights of tars produced in atmospheric pressure conditions are similar to those produced in devolatilization of the same coal in the UTRC-EF and the initial tars produced in the PSU-EF before significant gas phase reactions pyrolytically crack the tars to lower molecular weight characteristics.

The UTRC-HG data, however, reveals an aspect of the tar evolution process not readily apparent in the EF data -- the influence of ambient pressure on volatile yield characteristics. Increasing the pressure from vacuum to one atmosphere decreases the tar yield while increasing the light gas and char yields. Lower molecular weight tars are evolved under pressure, relative to vacuum conditions (See Table VI). CH_4, CO and C_2H_4 gas yields are approximately doubled in changing from low pressure to one atmosphere devolatilization conditions. However, evidence of high temperature tar pyrolysis reactions are not apparent as C_2H_2 and HCN yields are not significantly changed by a change in extrinsic pressure alone. The ambient pressure inhibits release of some of the heavier tar species. Longer times in the grid hot zone result in low temperature pyrolysis reactions, consisting mainly of methylene bridge and alkyl and oxygen functional group decompositions. These reactions reduce the molecular weights and change the chemical characteristics of the heavy tars so that they are able to vaporize. Ring rupture reactions are not competitive at these temperatures, wherein the tars are quickly transferred through the narrow hot zone of the reactor. Consequently, C_2H_2 and HCN yields are low in such heating conditions.

To simulate higher heating rates, that is, pfc heating conditions, the UTRC-FL system was developed (Figures 13, 14). Figure 15 displays a typical flash pulse shape. The time-resolved pulse shape does not vary with the flash pulse conditions employed in this investigation, although the peak irradiance delivered to the coal samples placed on a glass slide within the reactor does.

The flash tube is operated in the low power output mode to minimize the UV components of the Xenon spectral output. In addition, pyrex glass is used for both reactor and neutral density filter sections, further reducing UV throughput to the sample. Figure 16 displays the measured spectral output from a typical set of flash pulse conditions.

Figures 17-20 display estimated temperature histories, time-averaged incident power densities for particle temperatures above 300°C, peak incident power densities, and product distributions for two different particle sizes of PSOC 1451D in the different ambient atmospheres. Again, the data indicate that the major tar release occurs very early in the devolatilization process and dominates the particle mass release even under very rapid heating conditions. In agreement with the UTRC-EF and UTRC-HG results, the major tar release occurs during the transient particle temperature rise between 300 and 600°C. Also in agreement with the other reactor systems results, transient particle and particle-gas boundary layer temperatures below 700°C do not produce light gases symptomatic of high temperature, gas phase reactions of tars -- HCN and C_2H_2. Figure 19 is particularly informative with respect to the coupled transport and chemical kinetic nature of coal devolatilization product distributions. The figure indicates that low pressure devolatilization of 50 micron particles, under the given conditions, produces mainly tar and light gases symptomatic of low temperature char degassing, CH_4, C_2H_4, CO and CO_2 and, unmeasured, H_2O. In one atmosphere of argon under the same transient radiant pulse, tar remains the dominant

volatile product but at reduced levels relative to the low pressure conditions. In addition, appreciable amounts of C_2H_2 and HCN are produced. Similar to the heated grid, these results indicate some heavy hydrocarbons are inhibited from rapid escape by interphase mass transfer resistance introduced by the increased ambient pressure. Unlike screen heating, however, these heavy tars behave as if they experience gas phase temperatures of 700°C or above either inside the particle or in the gas-particle boundary layer around the particle. As in the entrained flow reactor, such gas temperatures induce C_2H_2 and HCN producing cracking reactions in the tars.

Molecular weight characteristics of tars produced in this mode of heating display consistently greater molecular weight moments relative to tars captured in the other reactors (Table VI). It was believed that this could be due to THF extraction of large, unvolatilized species from the char particles. However, hand separating char particles from the tar deposits before THF application had little effect on the molecular weight distribution characteristics of the tars. Thus the tars of larger molecular weight characteristics are ejected during the tar evolution phase in these heating conditions, relative to the more moderate heating conditions induced by the UTRC-HG or EF systems. Although power densities of nearly 100 watts/cm^2 are created at the particle surface in the PSU-EF reactor, the evolved tars are not rapidly quenched, but rather are evolved into hot ambient gases, wherein rapid cracking reactions are unavoidable.

The UTRC reactor systems demonstrate the phenomenological sequence of bituminous coal devolatilization is invariant with heating rate for incident heat fluxes of several tenths of a watt/cm^2 and above and wherein particles are heated to temperatures of 600°C or greater. Tar species dominate the initial particle mass loss and account for the greater fraction of the mass loss during the particle temperature rise to 600°C. The rate of tar mass loss appears directly proportional to the rate of heat transfer for particle temperatures between 300 and 600°C. One would expect variations in particle mass loss behavior in the PSU-EF reactor relative to the UTRC systems to reflect corresponding differences in transient heat transfer conditions.

Figure 21 displays the estimated heat flux rates and total energy delivered to 69 micron particles injected into the PSU-EF reactor having matched gas and wall temperatures of 800°C. Figure 22 displays the measured weight loss (ash-tracer) for various size cuts of PSOC 1451D using N_2 as the coal carrier gas and the main stream gas. Figures 23 and 24 show the effect of changing the carrier gas mix at the same reactor temperature for two different particle sizes of the same coal. Figure 25 shows the effect of a 200°C increase in reactor temperature on particle mass loss for 81 m particles and Figure 26 for 115 m particles.

In view of the UTRC reactor system results, particularly the flash lamp results, these rapid particle mass loss observations for the bituminous coal particles are expected. The transient net power densities during the particle

temperature rise from 300 to 600°C in the PSU-EF range from 10-90 watts/cm^2. Tar release times in the UTRC-HG are on the order of 300 msec or greater, depending on the programmed heating conditions. In the UTRC-EF, wherein net power densities are similar, similar tar release times are indicated. In the UTRC-FL wherein net power densities are on the order of several hundred watts/cm^2, the tar release times are on the order of tens of milliseconds. The PSU-EF data indicate the major tar release occurs before the first major weight loss measurement, even for the largest particles at the lowest reactor temperatures. The tar release is associated with the transient particle temperature rise, that is, the transient heat transfer process, and certainly occurs during the first 100 msec of residence time. Most probably, considering the devolatilization sequence, the tar release occurs during the first 50 msec of residence time, that is, during the transient particle temperature rise through 600°. In addition, changes in heat transfer related parameters -- particle size, inert gas mix, and reactor temperature -- qualitatively affect the rate of mass loss as expected.

The phenomenological sequence of bituminous coal devolatilization appears invariant with heating conditions and is represented in Figure 27 and 28. The figure indicates that phenomenologically a highly volatile bituminous coal consists of an organic substrate to which tar precursors are attached. The fundamental nature of the attachment process remains ill-defined but distribution of physical and chemical bonding is likely (9, 10). Heating the coal to 300°C initiates the detachment process by thermally disrupting the

bonding of some physically attached tar precursors, that is, those attached by hydrogen bonding and Van der Waal type interactions to the coal substrate. Further heating through particle temperatures of 450°C is needed to complete the physical detachment process as well as the chemical bond breaking processes.[9, 11] Heating the particles through 600° C requires enough energy to both complete the intra-particle tar formation processes and vaporize these heavy molecular weight species. The greater the heat transfer rate during this transient particle temperature rise, the greater the rate of tar evolution. The intra-particle tar precursor formation processes appear fast relative to the tar evolution processes, from a phenomenological point of view. Results from all experimental systems indicate that tar species dominate the initial mass loss of a bituminous coal and that the rate of mass loss varies directly with heat transfer related parameters.

Ambient pressure inhibits the release of the heaviest tar species that can evaporate in low pressure conditions, reducing total tar yields while increasing light gas and char yields. The low temperature (600°C) reactions induced by ambient pressure and which result in tar species having sufficient vapor pressure to evaporate, generate primarily H_2O, CH_4, CO and C_2H_4 gases. However, MWD's of evolved tars are also dependent on the rate of heat transfer at ambient pressure. The greater the heat transfer rate the greater the MWD's characteristics of the initially evolved tars. Rapid radiative transfer to coal particles appears to enhance desorption of large tar species in a manner not unsimilar to that observed in laser desorption mass

spectrometry investigations of large organic molecules (29-33). Thus, depending on the mode and power density conditions of heat transfer to bituminous coal particles during the tar mass loss phase, the tar evolution process may occur via vaporization, convective transport or a non-equilibrium, radiative induced desorption process.

Gas phase reactions of tars are rapid for gas temperatures of 700°C or greater. Such reactions result in reductions in the molecular weight moments of the THF soluble tars while generating large increases in C_2H_2, C_2H_4, CO and HCN gases. Entrained flow reactors in which wall and gas temperatures are matched create an environment in which such rapid gas phase reactions are unavoidable. Such reactions are also observed in the flash lamp reactor for conditions in which particle-gas bonding layers are expected to exceed 700°C during the tar evolution phase.

Figure 29 shows a typical sigmoid "weight loss" curve for devolatilization showing the distinct, but overlapping phases of devolatilization of Figures 27 and 28. Also listed are the parameters that appear to be rate-dominating in each phase. In each phase, thermal transport (q), mass transport (m) and chemical kinetic parameters contribute to the observable behavior, but one parameter type dominates weight loss rates. In each phase the phenomena responsible for rate control is underlined, while those making important coupled contributions are capitalized. Different parameter types dominate different phases of the weight loss process. Heat transfer dominates the main

tar formation and release, with mass transport and chemical kinetics heavily influencing the latter stages of tar release, that is, the heaviest species. Char degassing on the other hand appears to be dominated by chemical kinetic phenomena.

The important implications of Figure 29 are: weight loss rate phenomena for high tar yielding coals are dominated by transport parameters; devolatilization times vary directly with the conditions of heating because of the importance of heat transfer on tar evolution phase of the total process.

Engineering Kinetic Implications

For high tar yielding coals -- subbituminous and bituminous -- weight loss phenomena are not simply transport or chemically controlled. The dominating parameters vary with the stage of devolatilization. Such an understanding implies that global weight loss kinetic models developed to correlate data corresponding to experiments with different transport conditions should produce quite different rate constants. This is observed to be the case (1,2). Based on the operational understanding of devolatilization presented above, one would expect disparate weight loss kinetic constants because of large variances in transport conditions with experiment (1).

More positively, f thermal transport conditions dominate the rate of tar evolution for subbituminous and bituminous coals, then one should be able to

correlate tar evolution response times with a heat transfer parameter. Since tar species dominate the initial mass loss for such coals, this is equivalent to correlating the initial mass loss with a heat transfer index.

Using measurements of reactor flux profiles or estimated flux rates to particles during their 300-600°C temperature rise, one can estimate a time-averaged heating rate index for a given devolatilization experiment by:

$$\frac{\text{Ave. Flux Rate } \Big]_{\text{watts/cm}}^{300\text{-}600^\circ\text{C}}}{\text{Particle Size, cm}}$$

The 300-600°C temperature range restricts the correlation process to the first stage, the tar formation and evolution phases, of devolatilization, corresponding to the first 50-60% of the particle mass loss. The time response of the tar mass loss versus the heating rate index for a range of different experiments is shown in Figure 30. The data indicate the initial tar mass loss produced is directly related to heat transfer conditions. The range of experimental conditions spans three orders of magnitude in particle size and six orders of magnitude in heat transfer rate. From an engineering correlation perspective, the relationship is informative. From a chemical perspective, it can be misleading, since it has been demonstrated that the chemical characteristics of the tars change with transient heating conditions.

REFERENCES

1. Howard, J. B., in Chemistry of Coal Utilization, Sec. Supp. Volume (ed. M. A. Elliott) John Wiley & Sons, New York, 340 (1981).

2. Solomon, P. R. and Hamblen, D. G., DOE Report DE84000225, DOE-Morgantown Energy Technology Center (1983).

3. Solomon, P. R. and Colket, M. B., Fuel, 749 (1978).

4. Solomon, P. R., et al., Nineteenth Symp. (Intern.) on Combustion, The Combustion Institute, Pittsburgh, 1139 (1982).

5. Solomon, P. R., et al., American Chemical Society, Div. of Fuel Chemistry, 26, No. 3, 6 (1981).

6. Solomon, P. R., et al., Fuel, 65, 182, (1986).

7. Tyler, R. J., Fuel, 59, 218 (1980).

8. Doolan, K. R., et al., Fuel, 66, 572 (1987).

9. Fong, W. S., et al., Fuel, 65, 195 (1987).

10. Fong, W. S., et al., Fuel, 65, 25 (1987).

11. Campbell, J. H., Fuel, 57, 217 (1978).

12. Arendt, P. and van Heek, K. H. Fuel, 60, 779 (1981).

13. Serio, M., et al., Ind. Eng. Chem. Res., 26, No. 9, 1931 (1987).

14. Carangelo, R. M., et al., Fuel, 66, 960 (1987).

15. Gibbins-Natham, J. and Komdiyoti, A., Amer. Chem. Soc. Div. of Fuel Chem. Preprints, 32, No. 3 (1987).

16. Arendt, P. and van Heek, K. H., Fuel, 60, 779 (1981).

17. Present Investigation: UTRC-HG.

18. Peters, W. and Bertling, H., Fuel, 44, 317 (1965).

19. Present Investigation: UTRC-EF.

20. Present Investigation: UTRC-FL.

21. Hertzberg, M., et al., Amer. Chem. Soc.-Div. of Fuel Chemistry, 32, No. 3, 8 (1987).

22. Ballantyne, A., et al., Final Report DOE/PC/30291-6, DOE/PETC (1983).

23. Gat, N., et al., Final Report DOE/PC/40273-4, DOE-PETC (1983).

24. Granger, A. F. and Ladner, W. R., Fuel, 49, 17 (1970).

25. Ubayakahar, S. K., et al., Sixteenth Intern. Symp. on Combustion, The Combustion Institute, Pittsburgh, PA, 427 (1977).

26. Badzioch, S. and Hawksley, P. G. W., Ind. Eng. Chem. Process Design Div., 9, No. 4, 521 (1970).

27. Koloyashi, H., et al., Sixteenth Intern. Symp. on Combustion, The Combustion Institute, Pittsburgh, PA, 411 (1977).

28. Maloney, D. and Jenkins, R. G., Twentieth Intern. Symp. on Combustion, The Combustion Institute, Pittsburgh, PA, 1435 (1985).

29. Posthumus, M. A., et al., Analytical Chemistry, 50, No. 7, 985 (1978).

30. Beuhler, R. J., et al., Jr. Amer. Chem. Society, 96, No. 12, 3990 (1974).

31. Stoll, R. and Rollgen, F. W., Org. Mass Spec., 14, No. 12, 642 (1979).

32. Kistenaker, P. G., Adv. Mass Spec., 8A, 928 (1980).

33. Van der Peyl, G. J. Q., et al., Intern. Jn. Mass Spect. and Ion Physics, 42, 125 (1982).

Table I

Heat Transfer Characteristics of Reactors

Reactor	Conditions	Modes of Heat Transfer	Magnitude (w/cm^2)	Measurement Technique
UTRC-HG	Vacuum	Radiation	0.1-1.0	Measure current and voltage-compute power and normalize WRT to screen surface area
	1 atm helium	Radiation+ Conduction	0.1-1.0 1.0-4.0	
UTRC-EF	1 atm argon	Radiation+ Convection	2-25 0.1-5.0	Windowed and non-windowed water-cooled flux probes
UTRC-FL	Vacuum 1 atm argon	Radiation	100-1000	Rapid response pyroelectric detectors
PSU-EF	1 atm	Convection+ Radiation	50-100	Measure wall and gas temperatures and estimate power density to particle

Table II

ELEMENTAL COMPOSITION OF TARS

Temperature effects

HVA bituminous coal (PSOC 1451D)

Reactor wall (C)	Max gas (C)	20 - 30 microns %C	%H	%N	%(S + O)	H/C
790	350	84.05	6.07	1.64	8.24	0.87
840	400	84.07	5.94	1.67	8.32	0.85
930	510	84.37	5.86	1.68	8.09	0.83
		84.46	5.93	1.76	7.83	0.84
1020	665	84.62	5.55	1.69	8.14	0.78
1100	790	85.22	5.40	1.73	7.65	0.76
1190	890	85.55	5.27	1.74	7.44	0.74
1270	1000	86.00	5.08	1.73	7.19	0.71
Parent coal		82.42	5.35	1.57	10.65	0.79
		81.07	5.24	1.62	12.04	0.78

RA2419TX.004

Table III

ELEMENTAL COMPOSITION OF TARS

Temperature effects

Reactor wall (C)	Max gas (C)	63 - 75 microns %C	%H	%N	%(S + O)	H/C
790	350	83.97	6.22	1.64	8.14	0.89
930	510	84.47	5.83	1.72	7.98	0.83
		84.16	5.79	1.74	8.29	0.83
1270	1000	85.50	5.29	1.76	7.43	0.74
Parent coal		80.55	5.53	1.59	10.32	0.80
		81.86	5.43	1.66	11.02	0.80

RA2419TX.029

RELATIVE MOLECULAR WEIGHT CHARACTERISTICS OF TARS

Reactor temperature effects

Reactor	Wall temp. (C)	Pos. (cm)	Res. time (msec)	Part. dia. (μm)	Atm.	Average[1] power density (w/cm^2)	$\bar{M}_n$	$\bar{M}_w$
UTRC-EF	750	36	620	20-30	AR	0.2	438	641
	840	36	580			0.6	452	665
	930	36	520			1.5	481	719
	1020	36	470			2.8	491	743
	1100	36	420			4.2	518	801
	1190	36	385			5.1	509	803
	1270	36	360			5.8	506	807
PENN STATE-EF	900	8	40	64	N_2	80.0	485	698
	900	23	110			80.0	490	709
	900	56	250			80.0	382	560
	1000	8	40			105.	531	766
	1000	23	100			105.	406	596
	1000	56	230			105.	275	407

1. Average net power density delivered to an inert spherical particle over the interval from 300°C to 600°C particle temperature

RA2419TX.006

Table V

CTRC-HG Volatile Yields - HVA Bituminous Coal

w% (DAF relative to specific sample)

T_f(C)	Programmed $\dot{T}$	t(sec)	Tar	CH_4	C_2H_6	C_2H_4	C_2H_2	HCN	CO	Ambient Atmosphere
800	1000	2.5 sec	24.8	2.18	0.63	0.25	0	0.20	1.41	760 mm argon
			26.2	2.08	0.55	0.25	0	0.19	1.19	760 mm argon
			23.9	2.01	0.49	0.26	0	0.12	1.30	760 mm argon
			34.7	1.26	0.42	0.13	0	0.09	0.73	Vacuum
			30.0	1.45	0.44	0.18	0	0.12	1.03	Vacuum
			31.4	1.08	0.38	0.10	0	0	0.51	Vacuum
390	1000	10	6.4	0	0	0	0	0	0	760 mm helium
500	1000	10	14.8	<0.05	<0.05	0	0	0	<0.05	760 mm helium
560	1000	10	15.3	0.22	0.11	0	0	0	0.08	760 mm helium
580	1000	10	27.2	0.30	0.17	0	0	0	0.11	760 mm helium
580	1000	10	23.7	0.34	0.15	0	0	0	0.16	Vacuum
580	1000	10	25.2	0.33	0.12	0	0	0	0.11	Vacuum

TABLE VI

TAR YIELDS AND MOLECULAR WEIGHTS

REACTOR/ PARAMETERS	PARTICLE SIZE [m]	ATM.	POWER DENSITY [W/CM^2]	Mn	Mw	% TAR YIELD	RUN I.D.
HG 450/2 *	49	VAC	0.62	626	839	14.2	229B
HG 550/2	49	AR	0.74	510	703	14.9	238A
HG 600/10	49	VAC	0.88	594	775	25.1	239A
HG 550/2	49	VAC	0.94	664	960	35.3	232C
HG 600/10	49	HE	1.3	522	692	12.7	242A
HG 350/1	49	VAC	1.8	655	948	20.0	224B
HG 800/2.5	49	VAC	1.9	621	855	21.0	221A
HG 800/2.5	49	VAC	1.9	610	843	24.4	237B
HG 800/2.5	254	VAC	2.0	639	869	25.1	246A
HG 800/2.5	127	VAC	2.1	616	841	28.4	245A
HG 800/2	774	VAC	2.3	616	875	24.3	253A
HG 800/2.5	774	VAC	2.3	632	869	23.3	247A
HG 800/2.5	49	AR	2.3	520	734	17.5	235C
EF 900/3 **	64	N2	50.0	485	698	****	017
EF 900/9	64	N2	-	490	709	-	018
EF 900/22	64	N2	-	382	560	-	019
EF 1000/3	64	N2	80.0	531	766	****	020
EF 1000/9	64	N2	-	406	596	-	021
EF 1000/22	64	N2	-	275	407	-	022
FL 1.8/30 ***	49	HE	225(32)	686	1059	6.0	705J
FL 1.5/60	49	HE	285(40)	784	1184	12.0	703C
FL 1.5/90	49	HE	430(60)	699	1134	19.0	704B
FL 2.2/60	49	HE	730(96)	545	898	17.0	706E
FL 1.8/30	49	AR	225(122)	714	1121	19.0	707C
FL 1.8/30	49	VAC	225	764	1180	23.0	709B
FL 1.5/60	49	VAC	285	663	1054	28.4	713B
FL 2.2/60	49	AR	729(293)	630	955	22.0	708B

Footnotes:

* HG X/Y - heated grid with 1000 C/sec ramp to X C, hold for Y sec, then 1000° C/sec ramp to 800°C, hold for 2.5-Y sec. The 600/10 runs are an exception: ramp to 600°C and hold for 10 sec.

** EF X/Y - entrained flow with X C gas temperature and Y" sampling position
900°C: 3"- 40 msec; 9" - 110 msec; 22" - 250 msec
1000°C: 3"- 40 msec; 9" - 100 msec; 22" - 230 msec

*** FL X/Y - flash lamp with X KV capacitor bank voltage and Y% neutral density filter. Values are time-averaged delivered irradiance; values inside parentheses are time-averaged net power density calculated from heat balance considerations. See Table III for characteristics of flash pulses.

***** - Not measured directly; at 3" residence time is estimated be about 20% (daf) of the parent coal mass from heated grid and flash lamp investigations. This yield represents the major fraction of the total volatile yields (Ref. 25) in 40 msec.

Figure 1

COAL COMBUSTION SEQUENCE

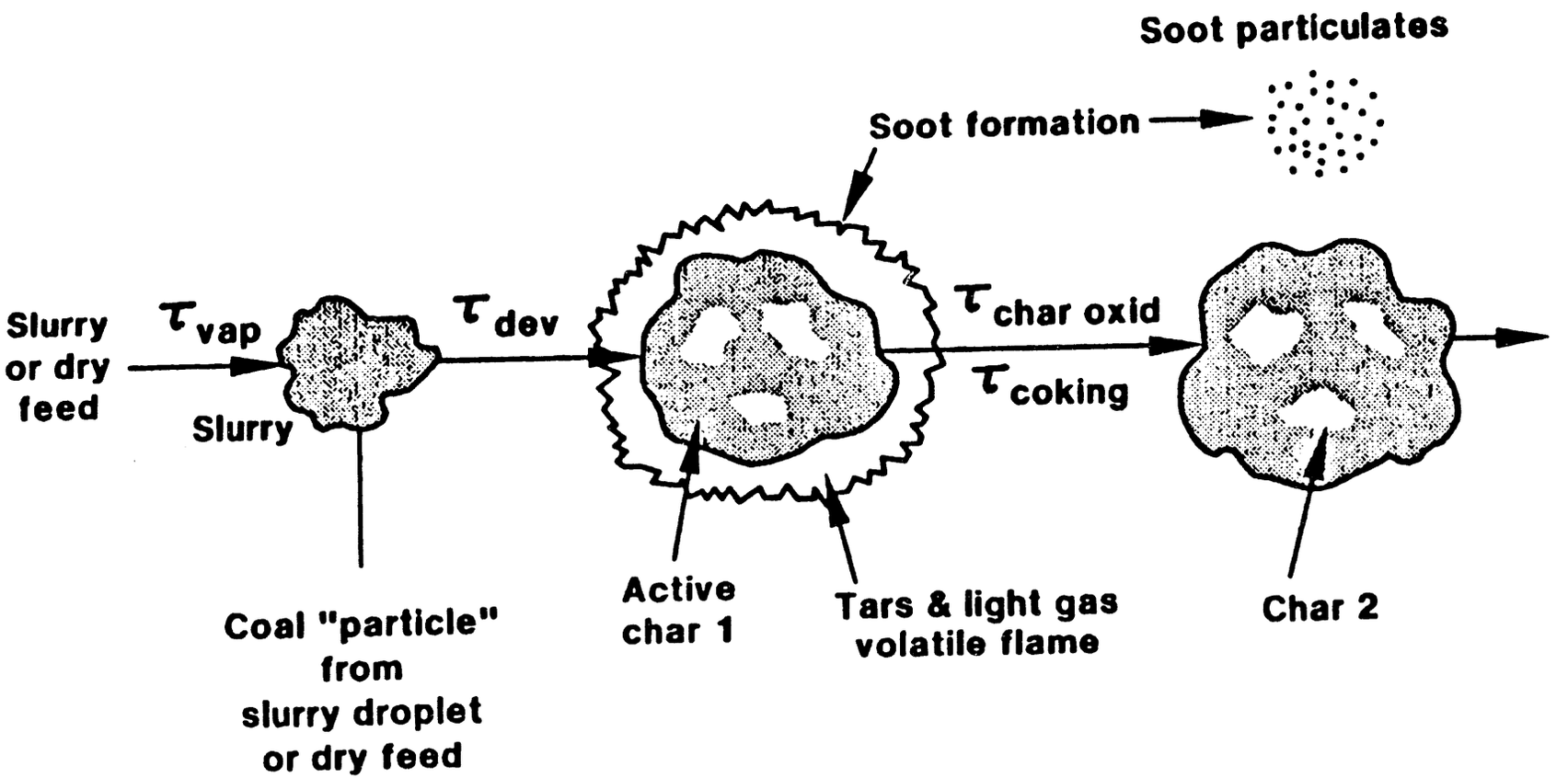

RA1132TX.015

Figure 2

H/C vs. (S+O)/C OF PSOC XXXXD COALS

20-30 microns, coals fed to UTRC EFR-cold flow, C_o capture

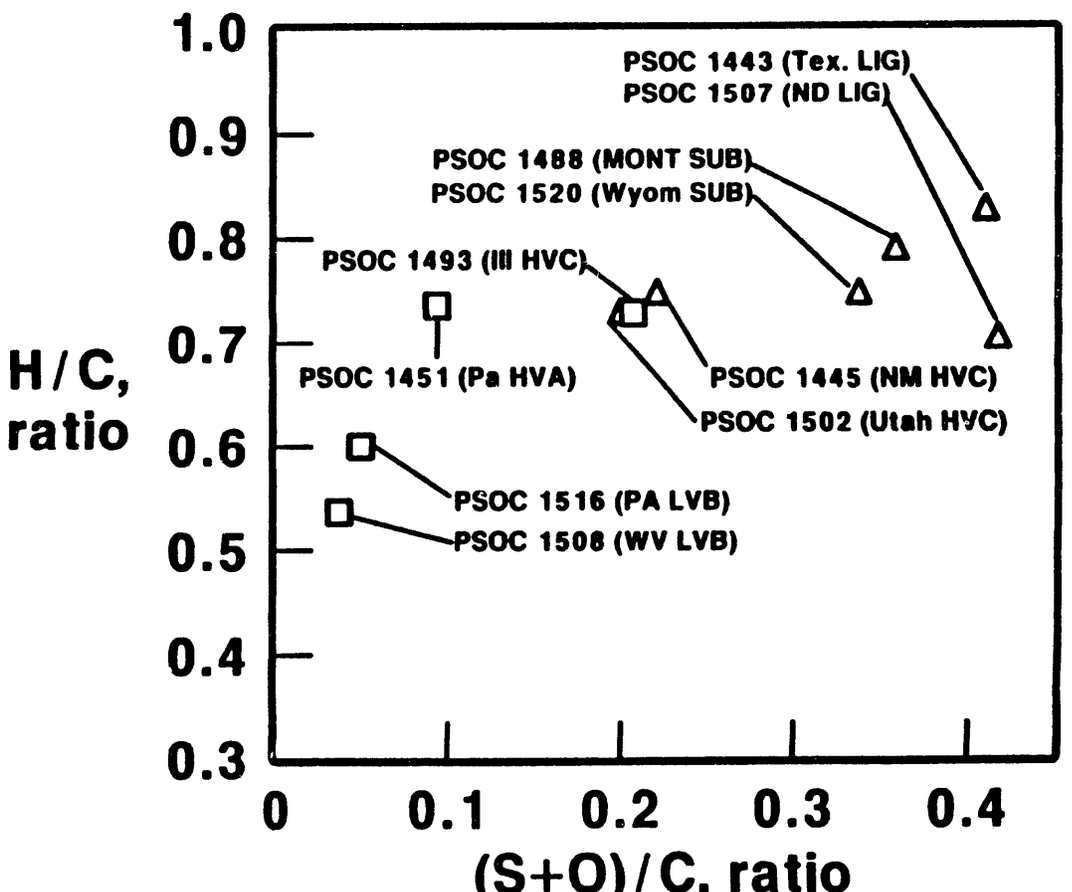

RA2415TX.017

Figure 3

REACTOR HEAT TRANSFER REGIMES

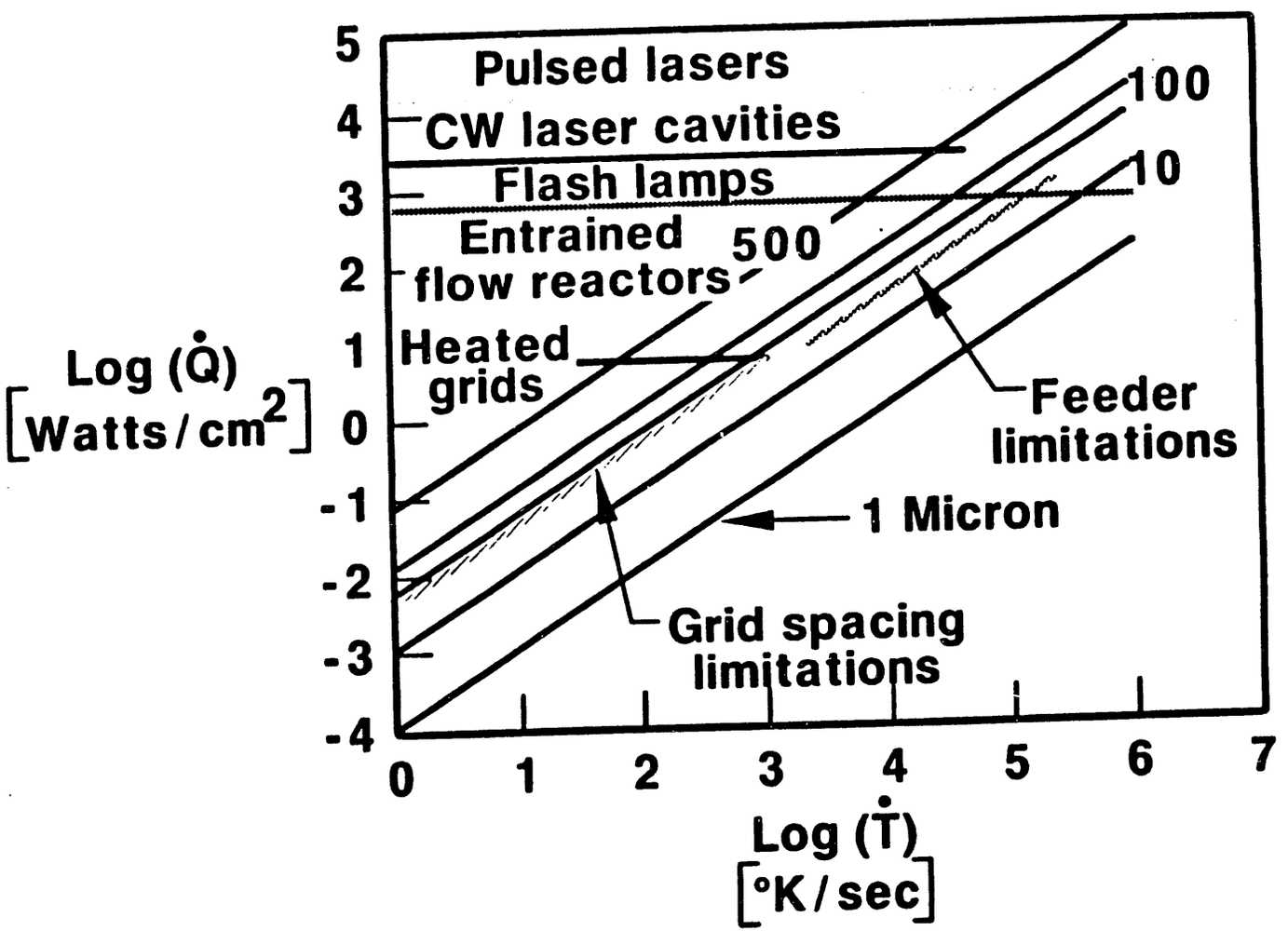

RA1784TX.003

Figure 4

ENTRAINED FLOW REACTOR FOR COAL DEVOLATILIZATION

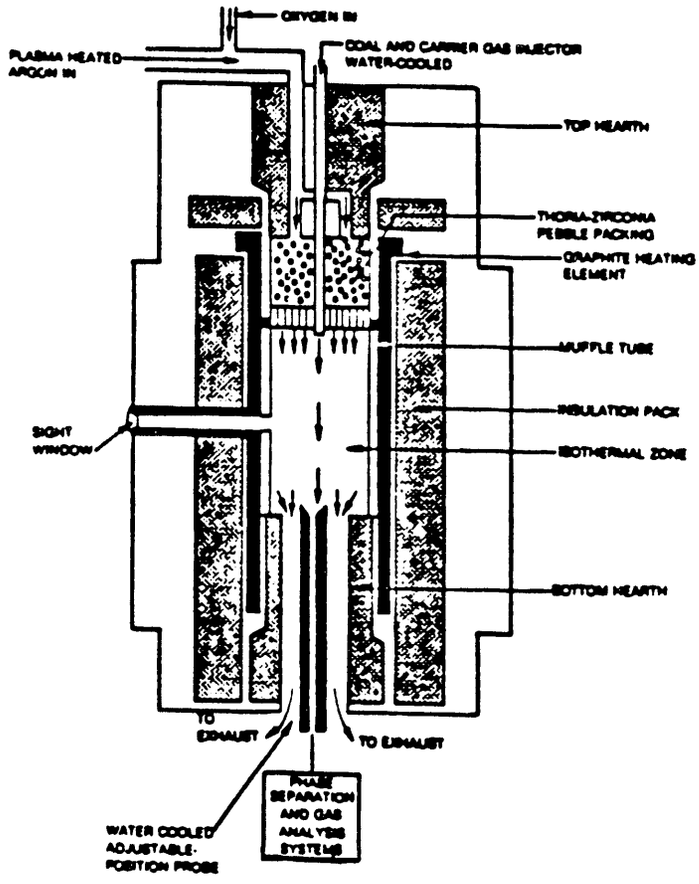

Figure 5

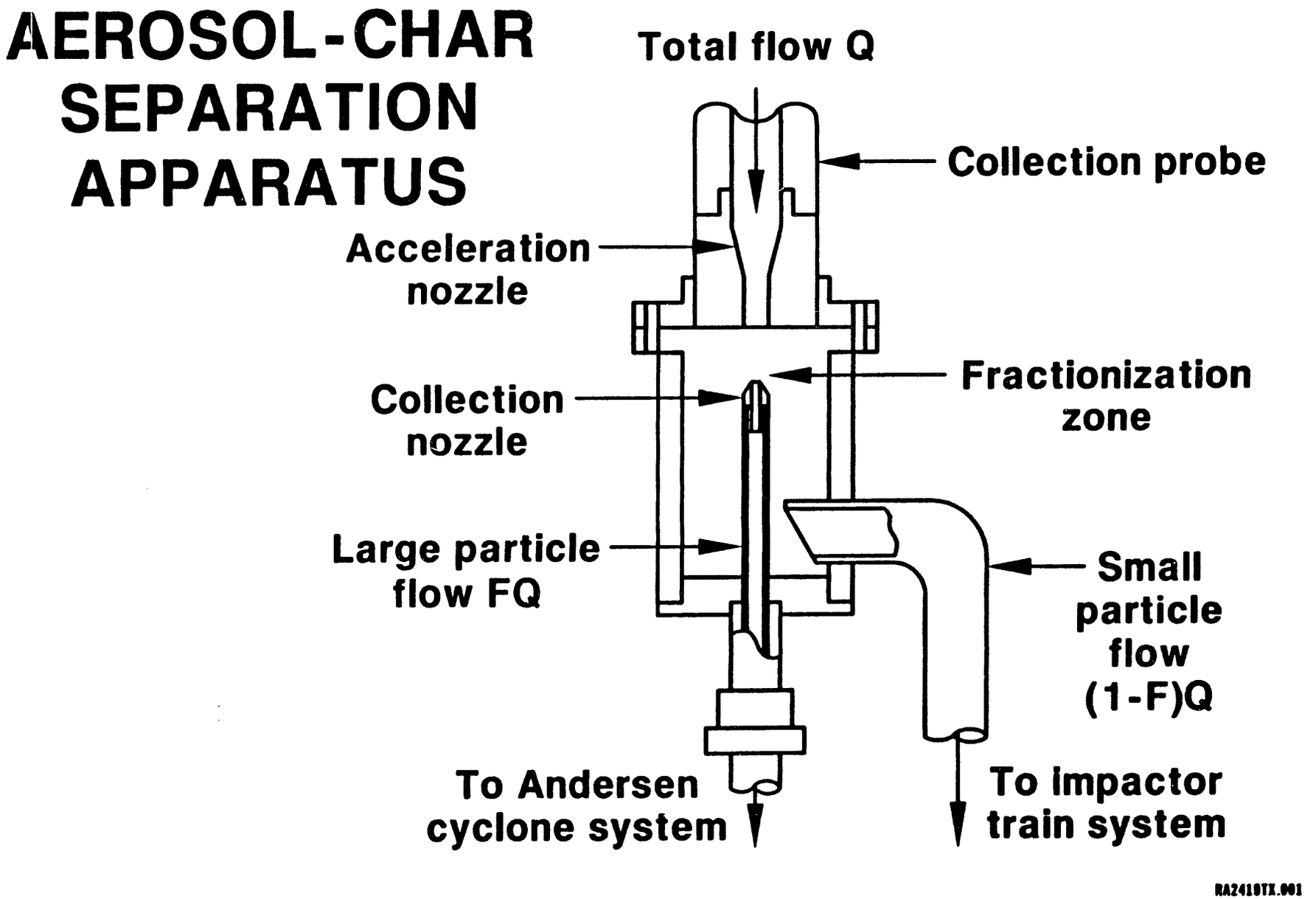
AEROSOL-CHAR SEPARATION APPARATUS
Total flow Q
Collection probe
Acceleration nozzle
Collection nozzle
Fractionization zone
Large particle flow FQ
Small particle flow (1-F)Q
To Andersen cyclone system
To impactor train system
RA2418TX.001

Figure 6

UTRC-EFR SAMPLE COLLECTION SYSTEM

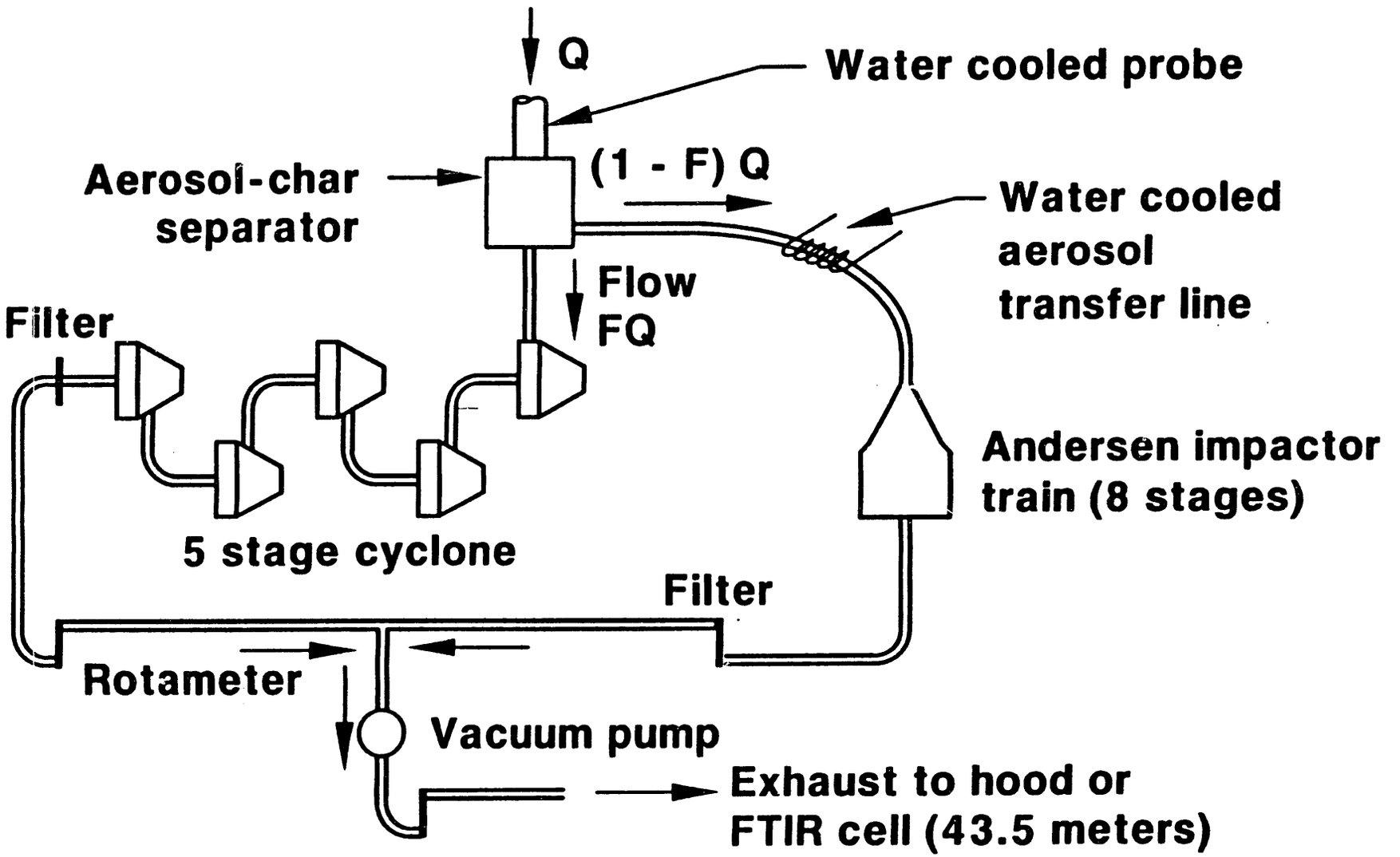

RA2419TX.002

Figure 7

UTRC-EFR REACTOR TOTAL FLUX PROFILES

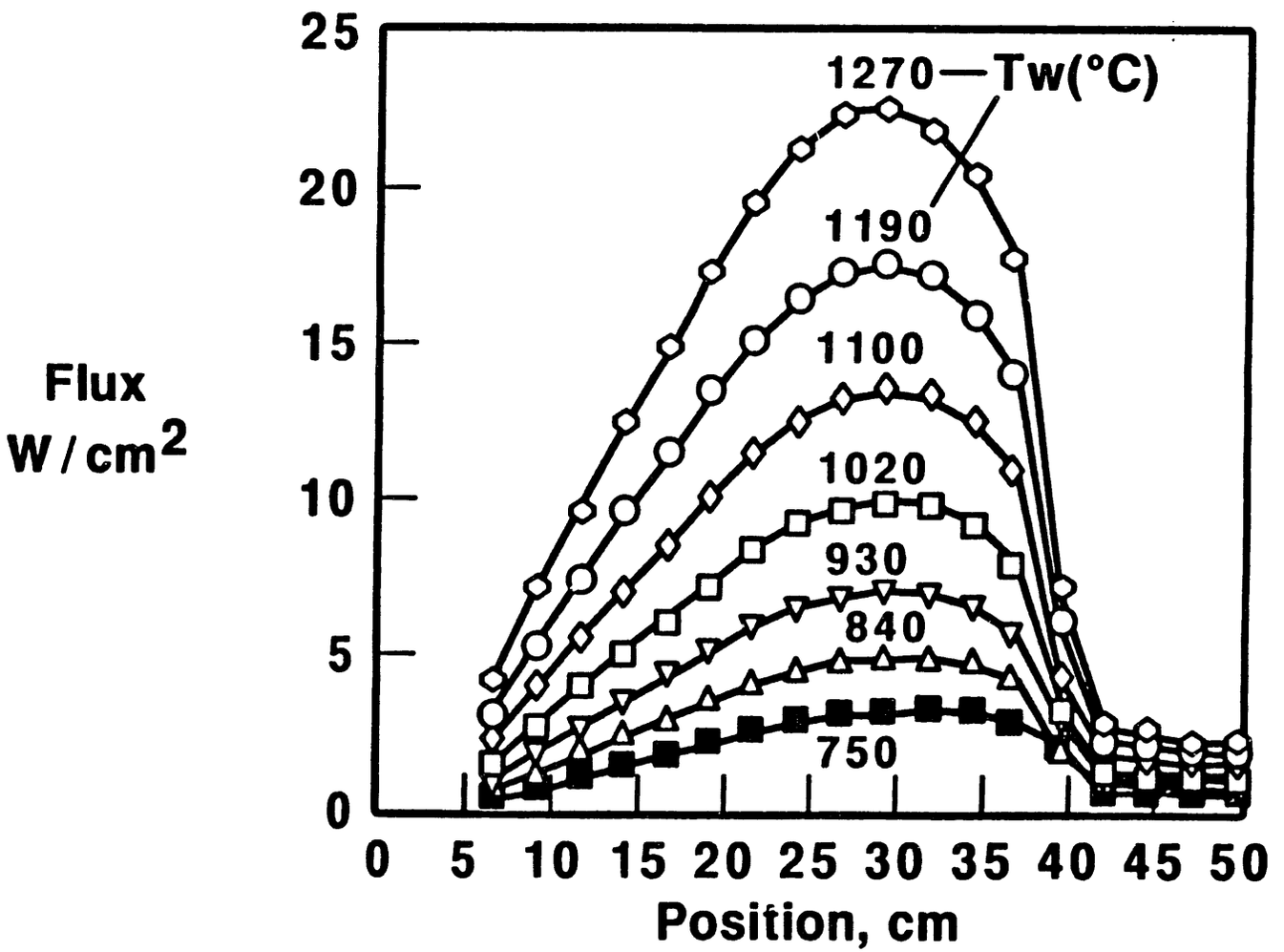

RA2415TX.001

Figure 8

UTRC-EFR REACTOR RADIATIVE FLUX PROFILES

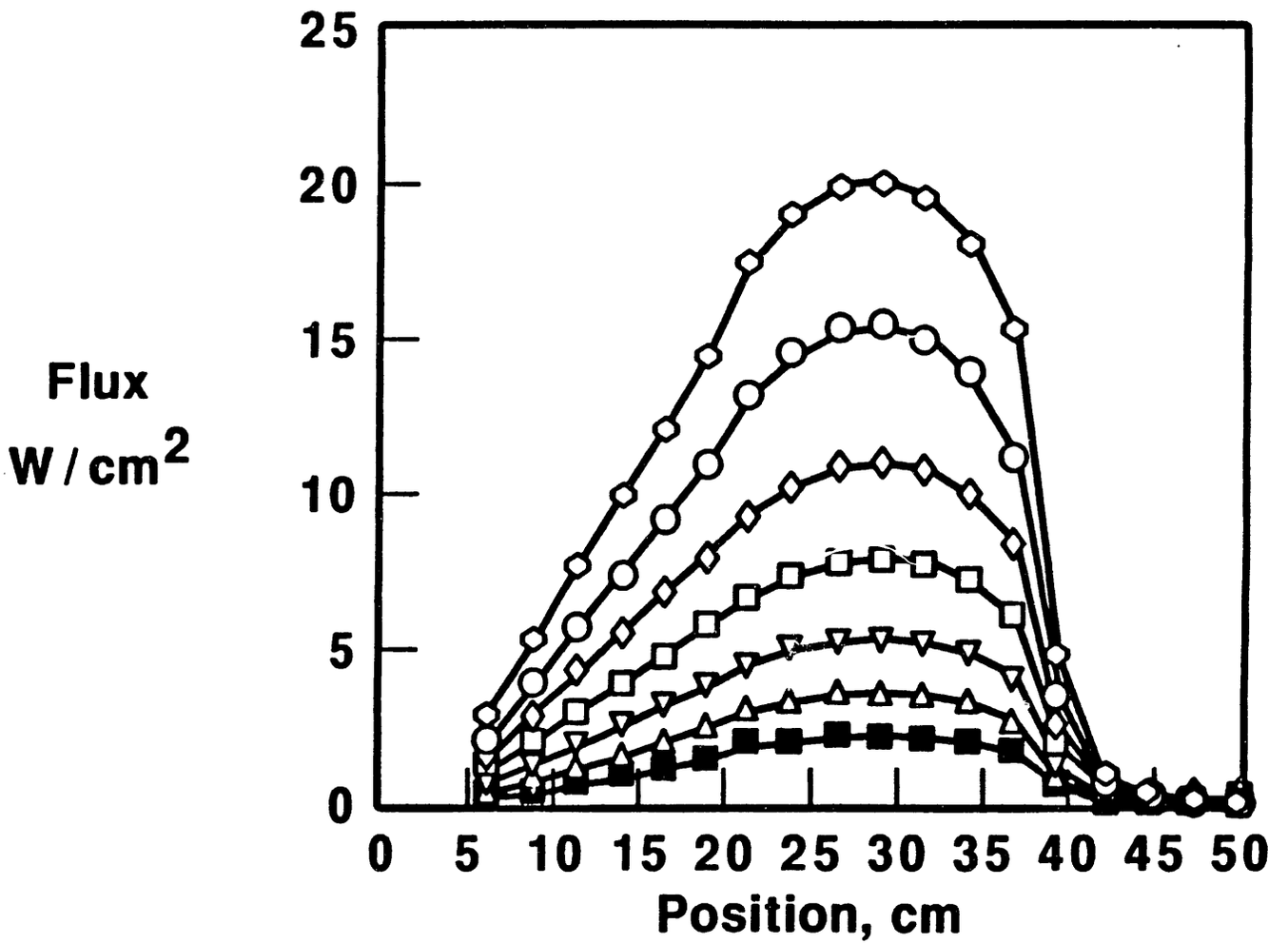

RA2415TX.002

Figure 9

UTRC-EFR COOLED PROBE 0.1016 CM BEAD DIA

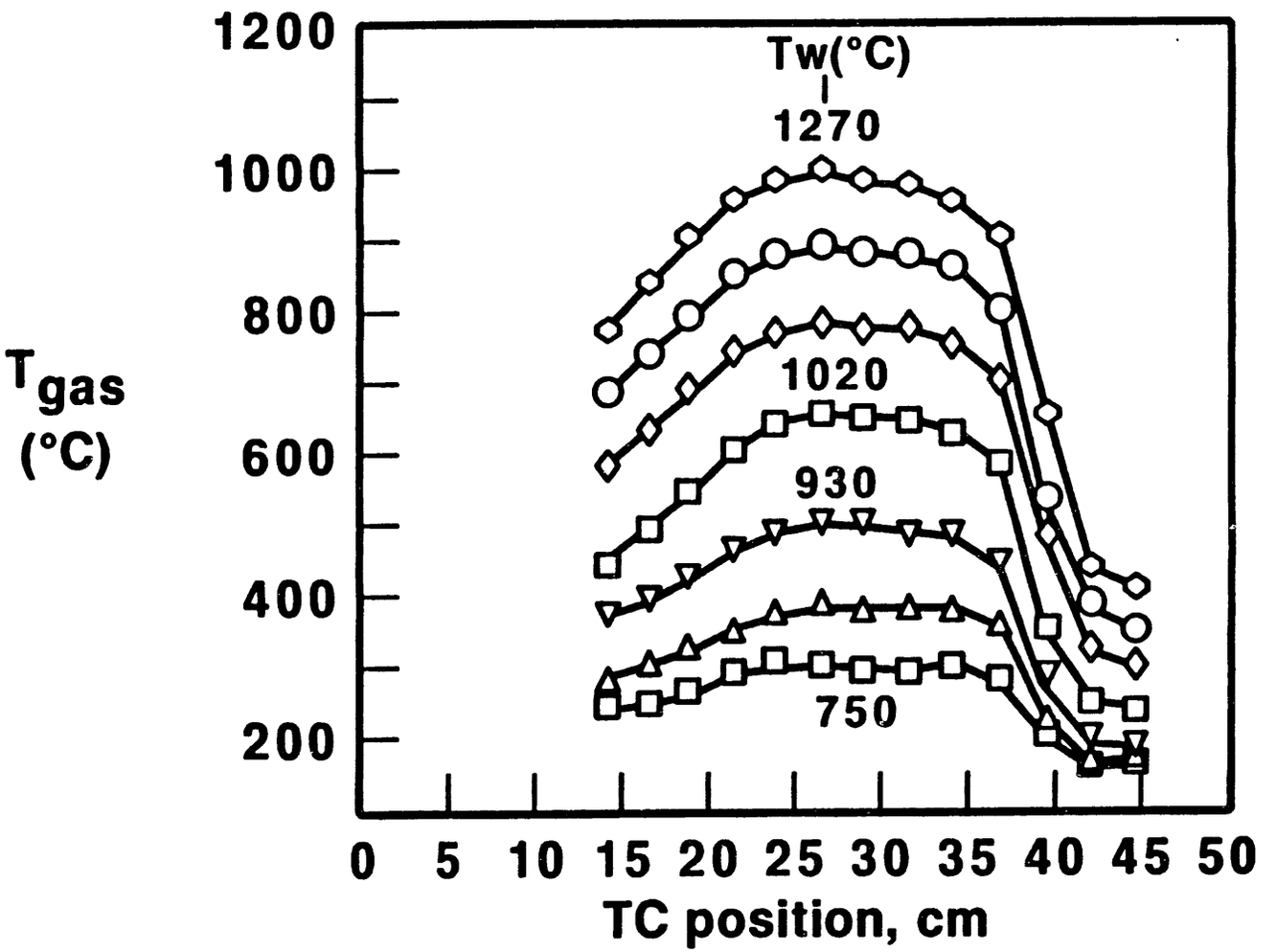

RA2415TX.003

Figure 10

MASS FRACTION VOLATILE YIELD vs. REACTOR WALL TEMPERATURE

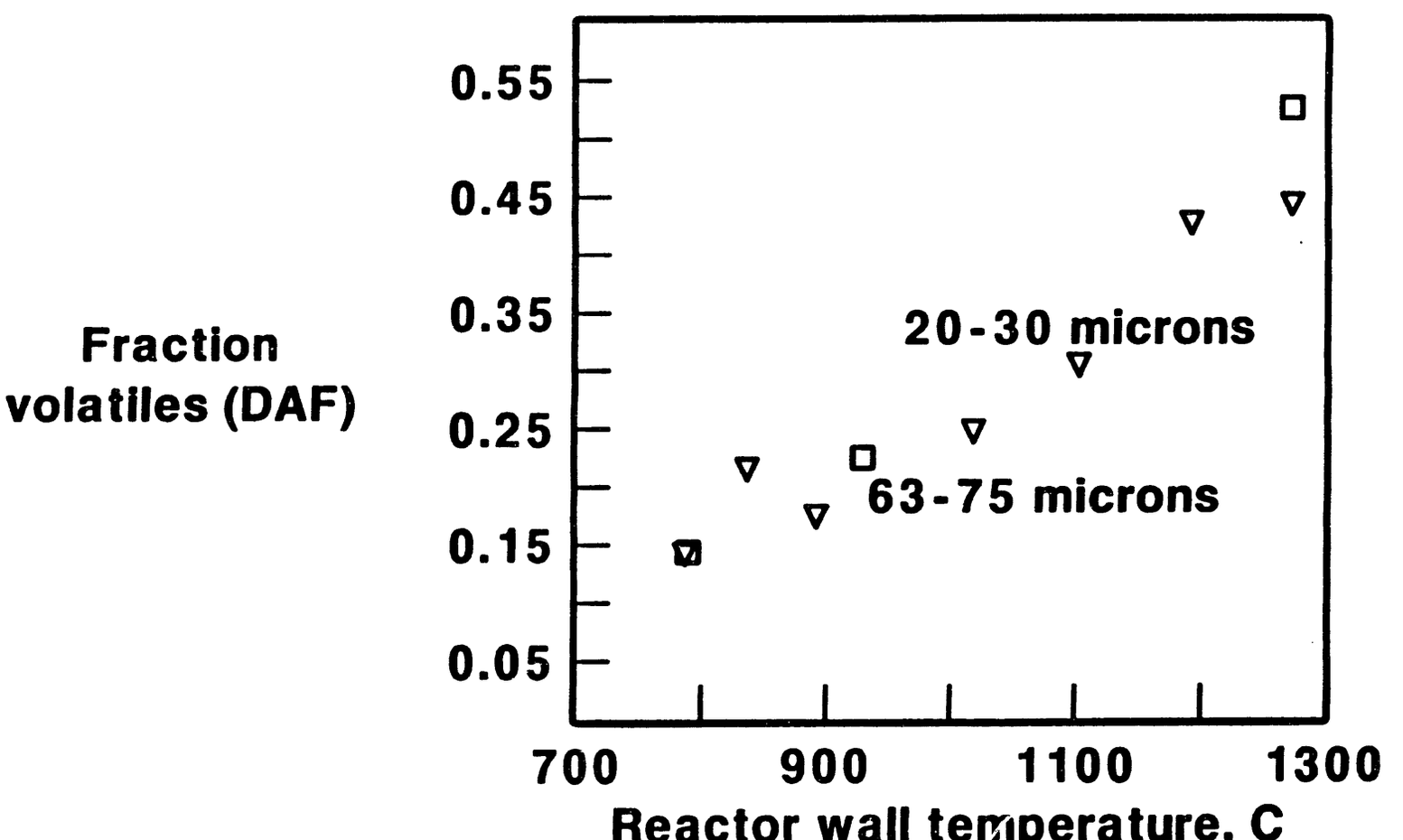

Figure 11

LIGHT GAS YIELDS vs. PEAK GAS TEMP. (C) PSOC 1451D, 20-30 MICRONS, 600 MSEC

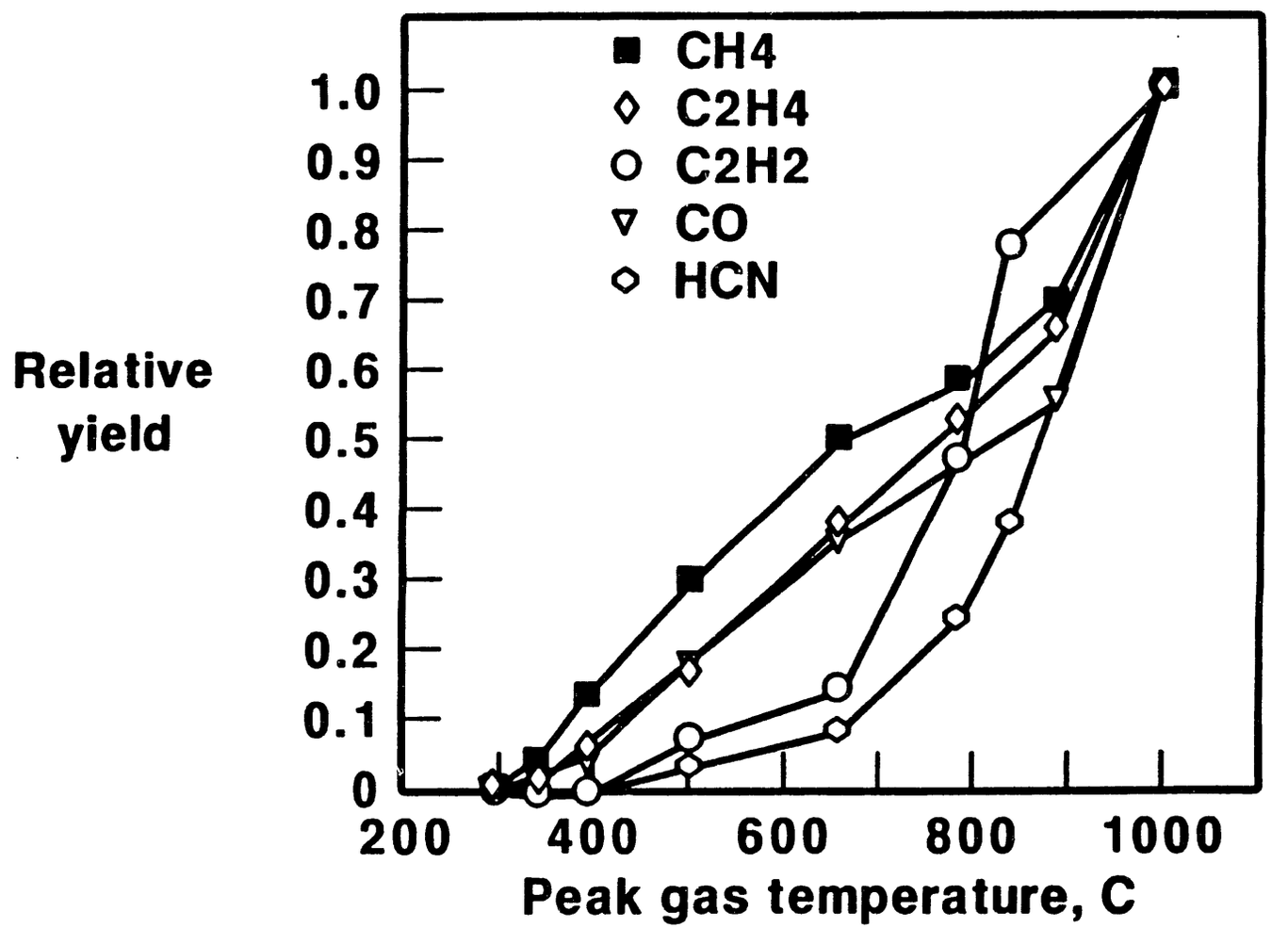

RA2415TX.005

Figure 12

HEATED GRID PSEUDO-STEADY STATE POWER LOSSES

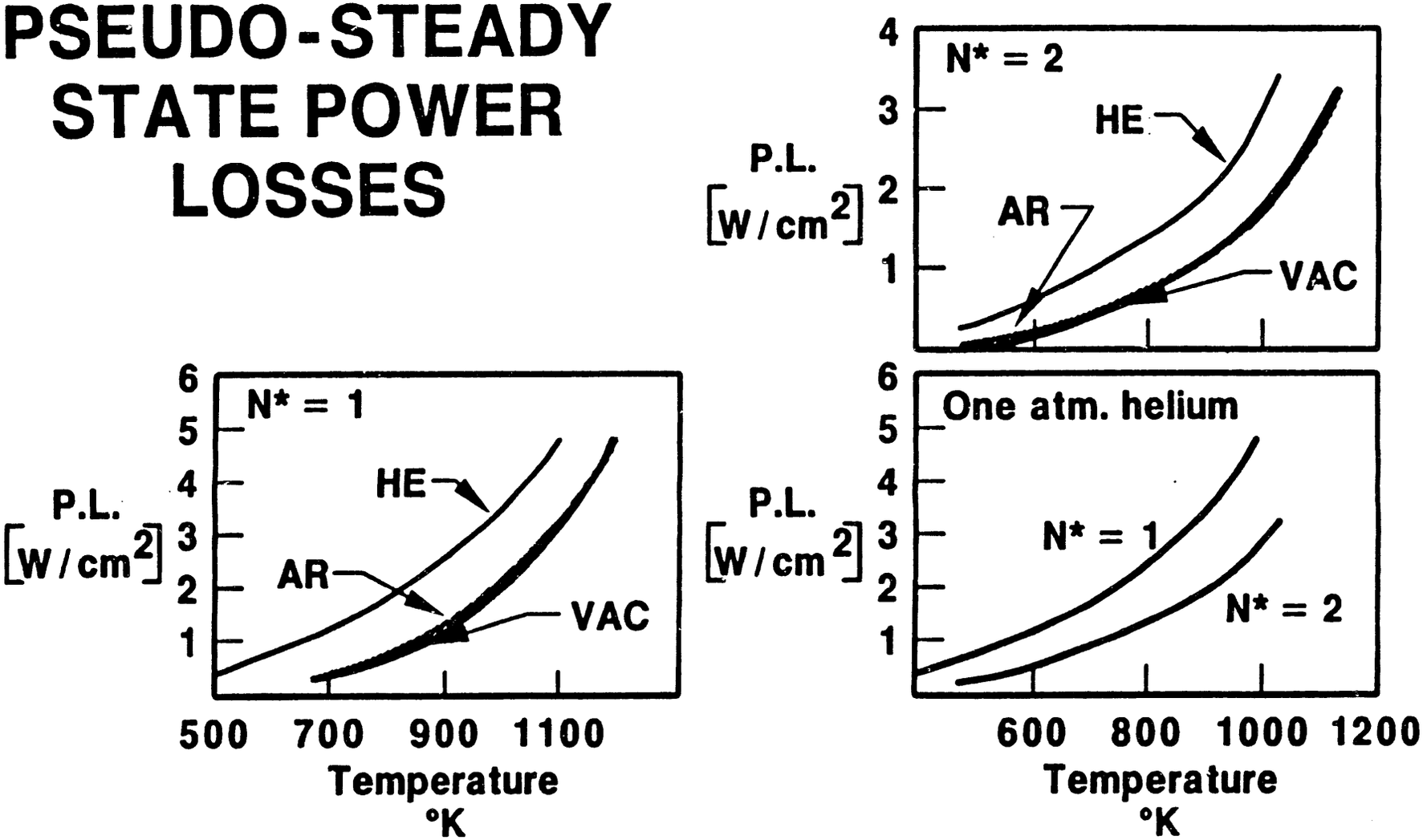

*N = number grid layers

RA1784TX.002

Figure 13

FLASH REACTOR AND GAS ANALYSIS SYSTEM

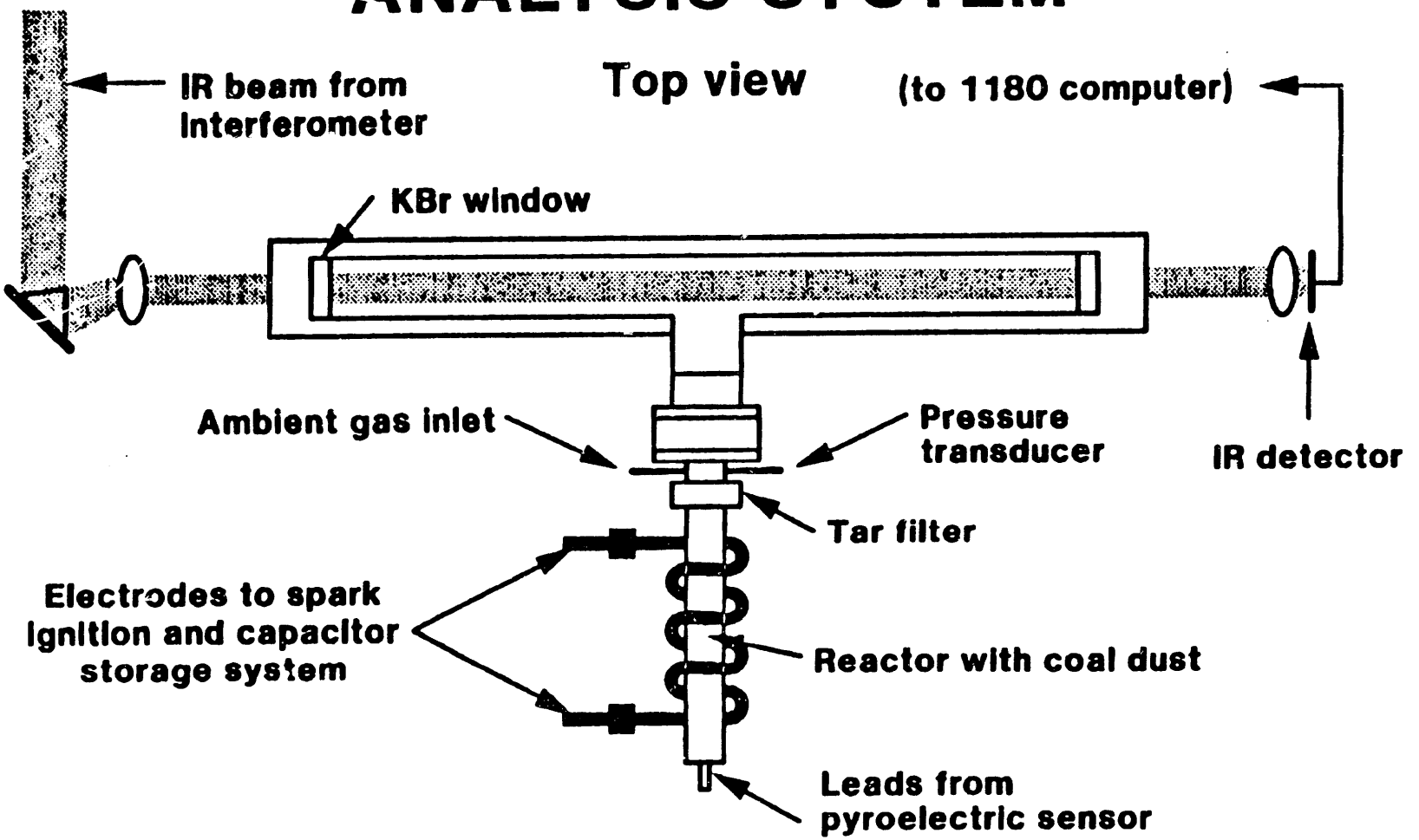

RA1132TX.009

Figure 14

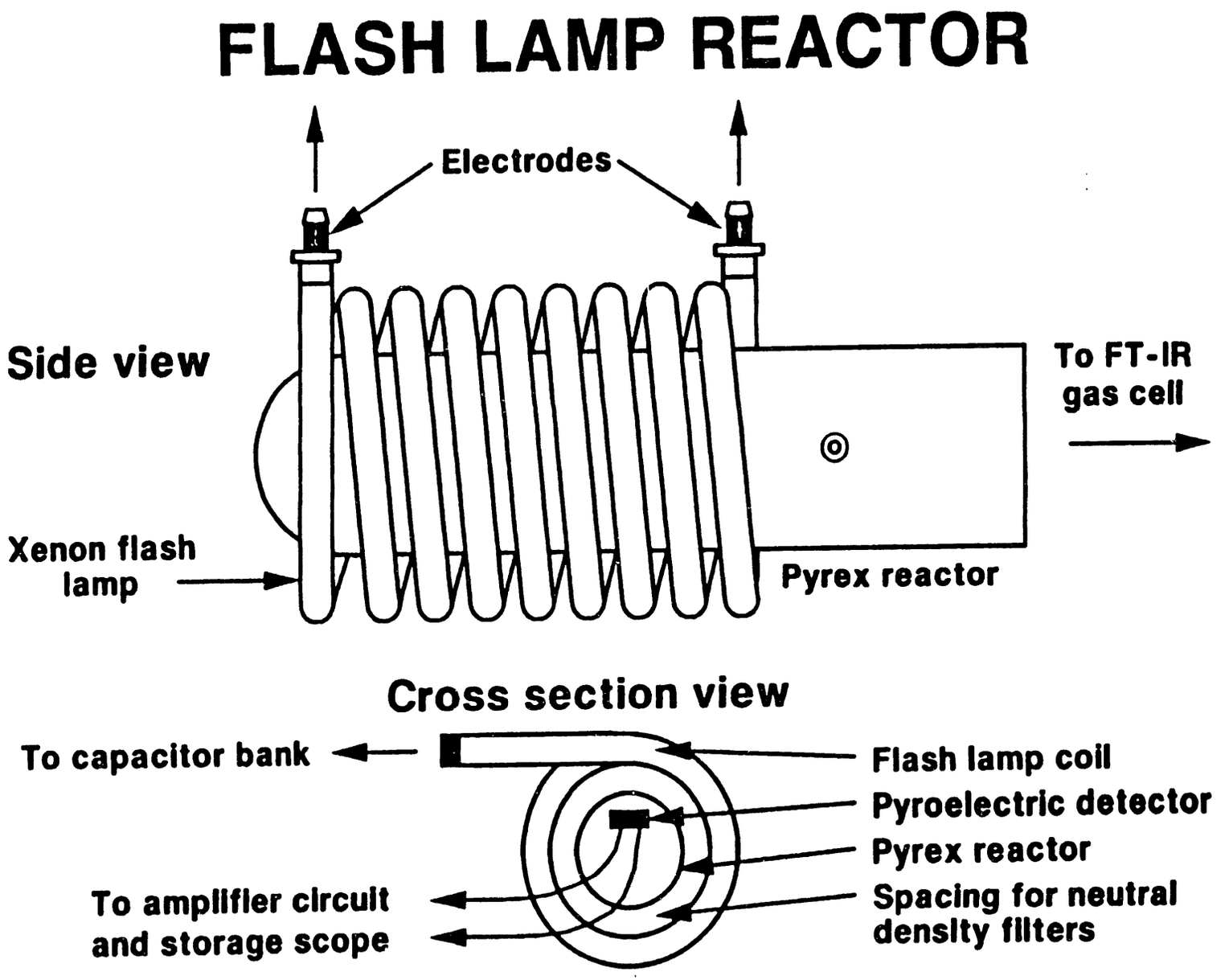
FLASH LAMP REACTOR
Electrodes
Side view
To FT-IR
gas cell
Xenon flash
lamp
Pyrex reactor
Cross section view
To capacitor bank
Flash lamp coil
Pyroelectric detector
Pyrex reactor
Spacing for neutral
density filters
To amplifier circuit
and storage scope
RA1132TX.008

Figure 15

FLASH LAMP PULSE SHAPE

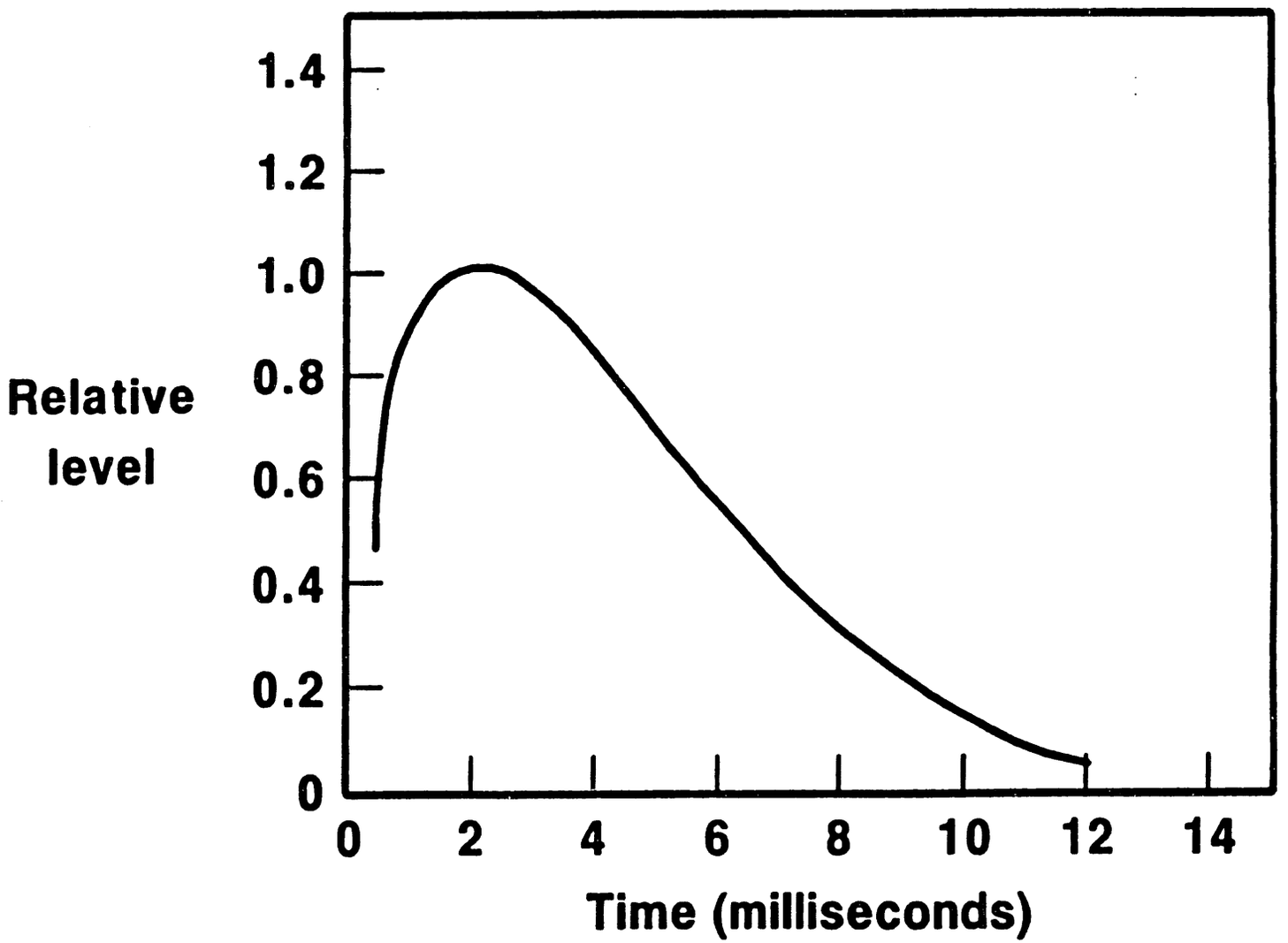

RA1784TX.004

Figure 16

FLASH LAMP SPECTRA

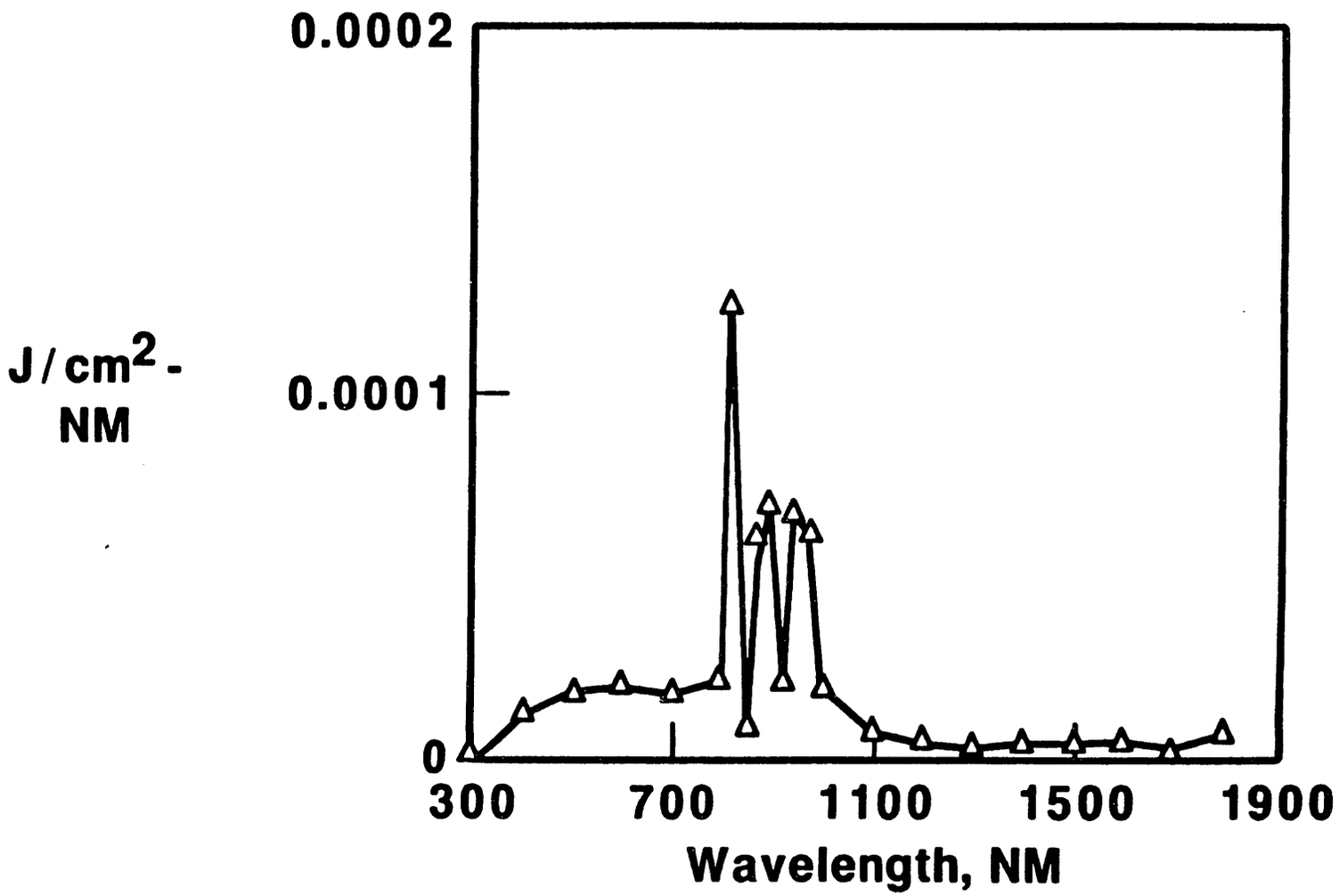

RA2415TX.007

Figure 17

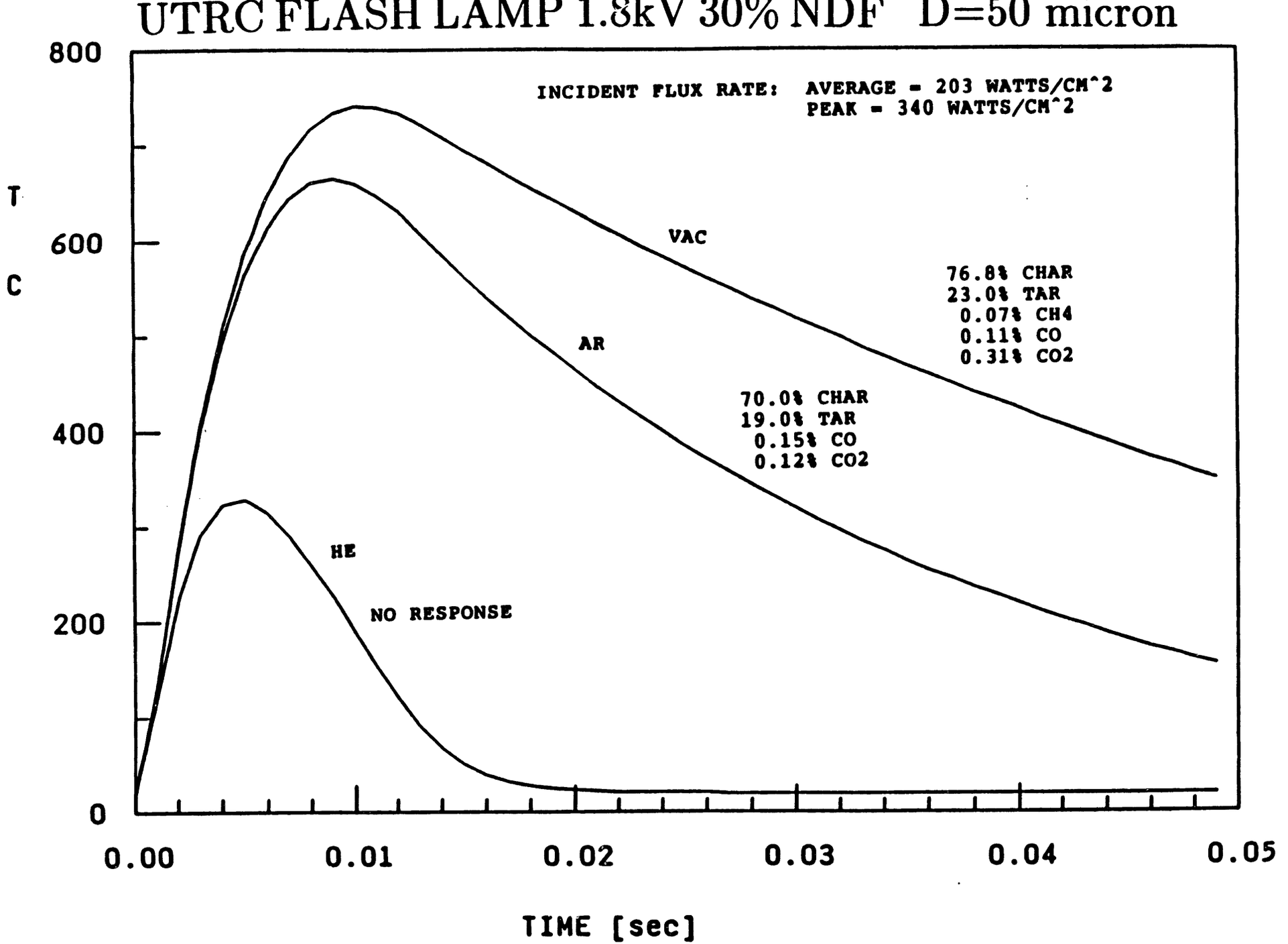
UTRC FLASH LAMP 1.8kV 30% NDF D=50 micron
INCIDENT FLUX RATE: AVERAGE = 203 WATTS/CM^2
PEAK = 340 WATTS/CM^2
VAC
76.8% CHAR
23.0% TAR
0.07% CH4
0.11% CO
0.31% CO2
AR
70.0% CHAR
19.0% TAR
0.15% CO
0.12% CO2
HE
NO RESPONSE
T
C
800
600
400
200
0
0.00
0.01
0.02
0.03
0.04
0.05
TIME [sec]

Figure 18

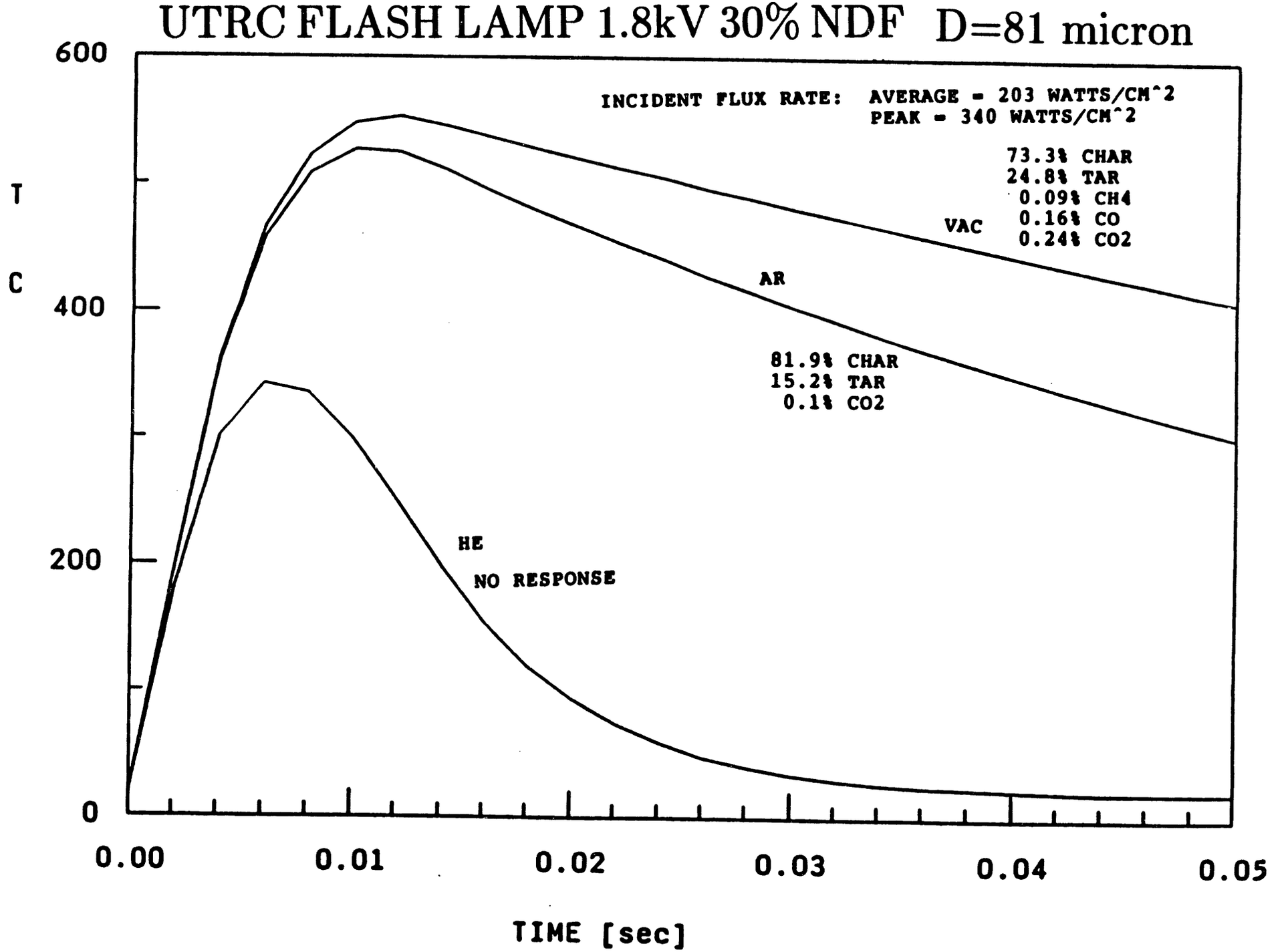
UTRC FLASH LAMP 1.8kV 30% NDF D=81 micron
INCIDENT FLUX RATE: AVERAGE = 203 WATTS/CM^2
PEAK = 340 WATTS/CM^2
73.3% CHAR
24.8% TAR
0.09% CH4
VAC 0.16% CO
0.24% CO2
AR
81.9% CHAR
15.2% TAR
0.1% CO2
HE
NO RESPONSE
T
C
600
400
200
0
0.00
0.01
0.02
0.03
0.04
0.05
TIME [sec]

Figure 19

UTRC FLASH LAMP

1.5KV 60% NDF D=50 micron

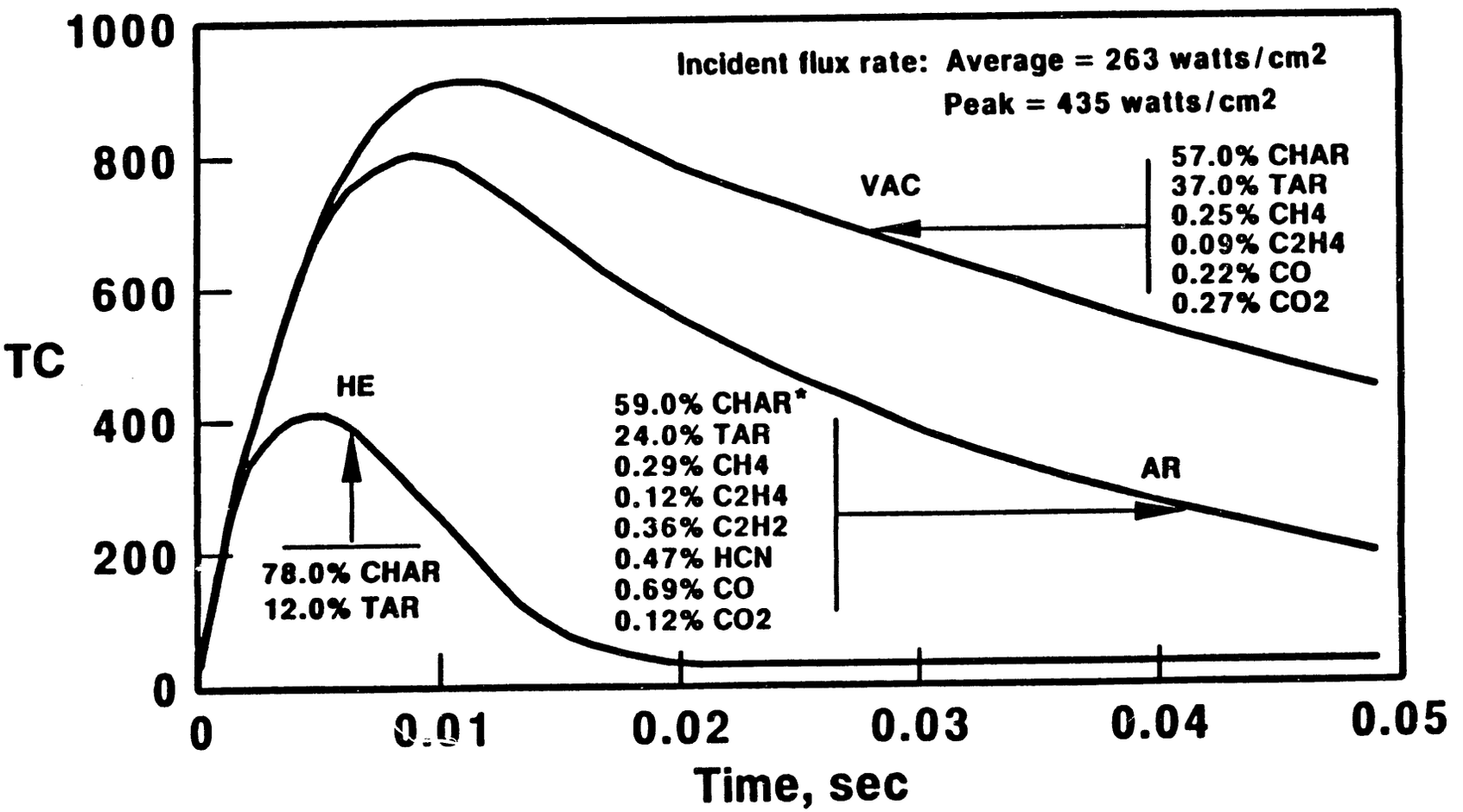

RA2415TX.006

Figure 20

UTRC FLASH LAMP 1.5kV 60% NDF D=81 micron

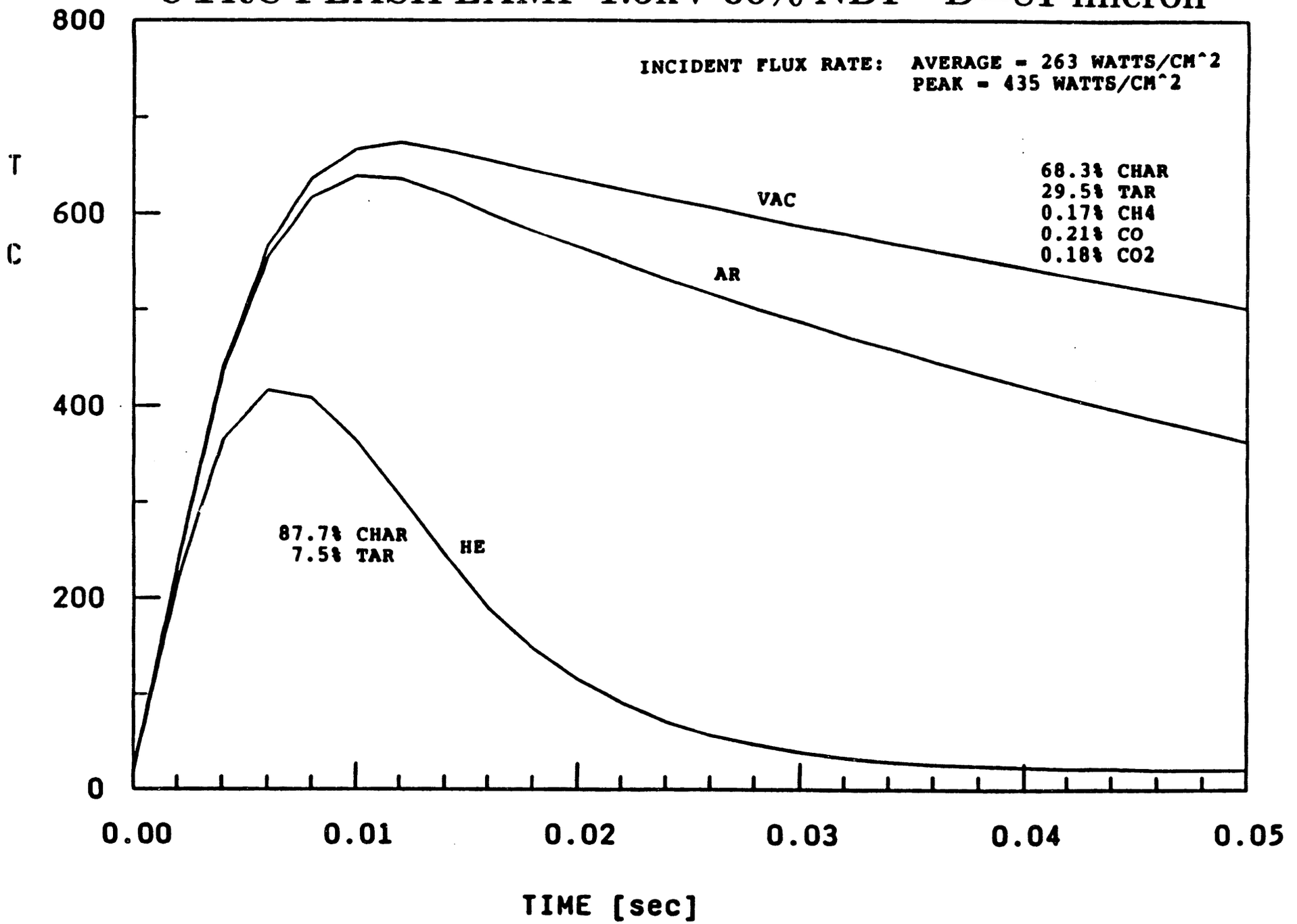

Figure 21

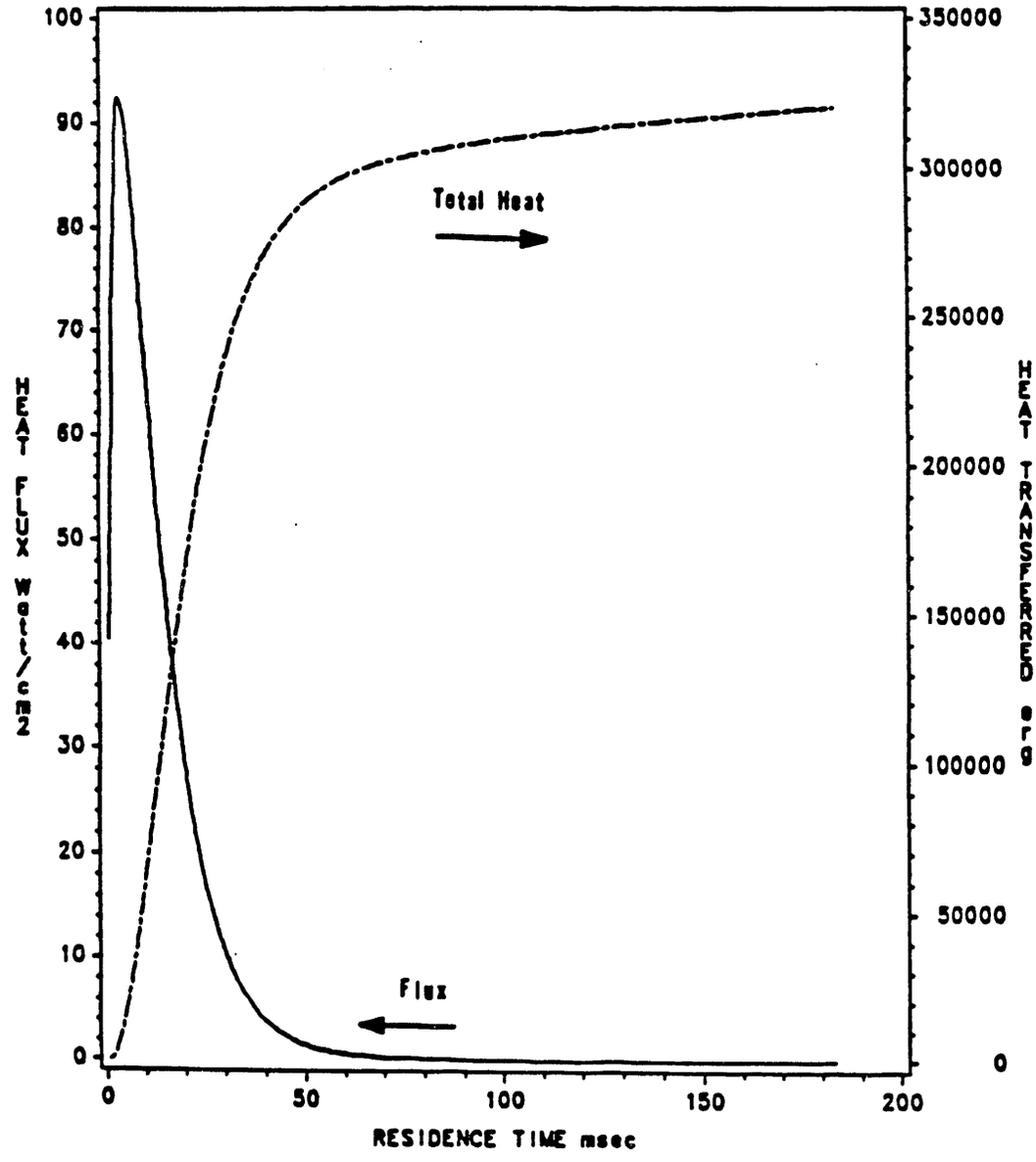

Heat Flux and Total Heat Transferred for 69 μm Coal Particles in a Nitrogen Atmosphere as a Function of Residence Time with a Reactor Temperature of 1073 K

Figure 22

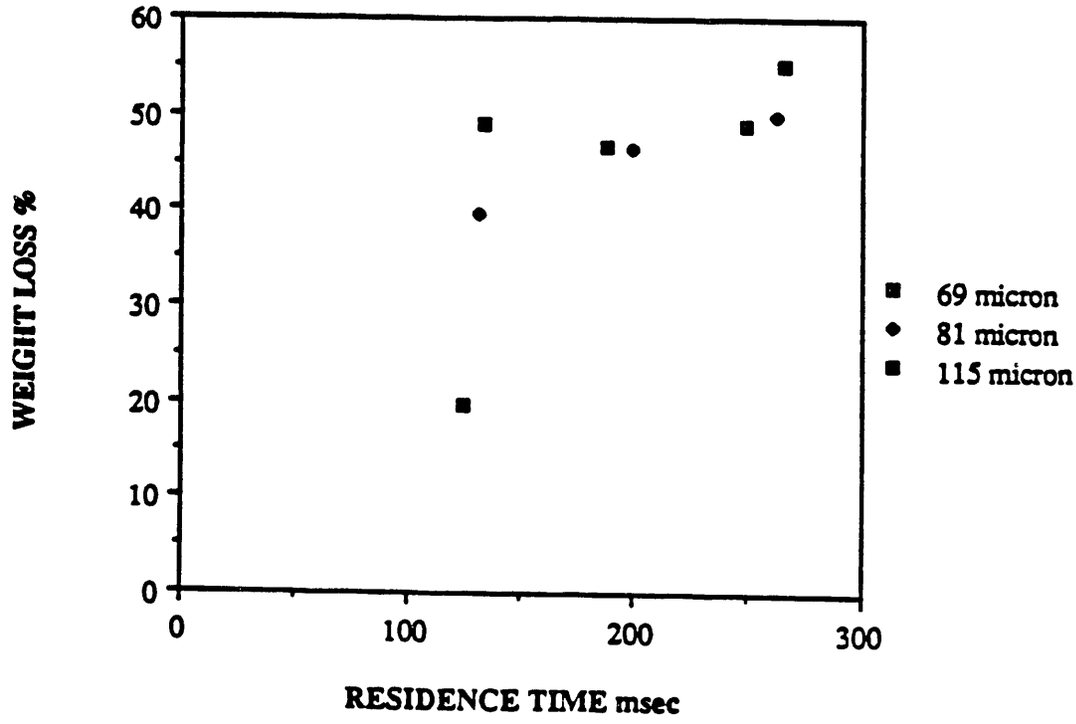

Effect of Particle Size on Weight Loss for PSOC-1451 at 1073 K in a N_2/N_2 Atmosphere

Figure 23

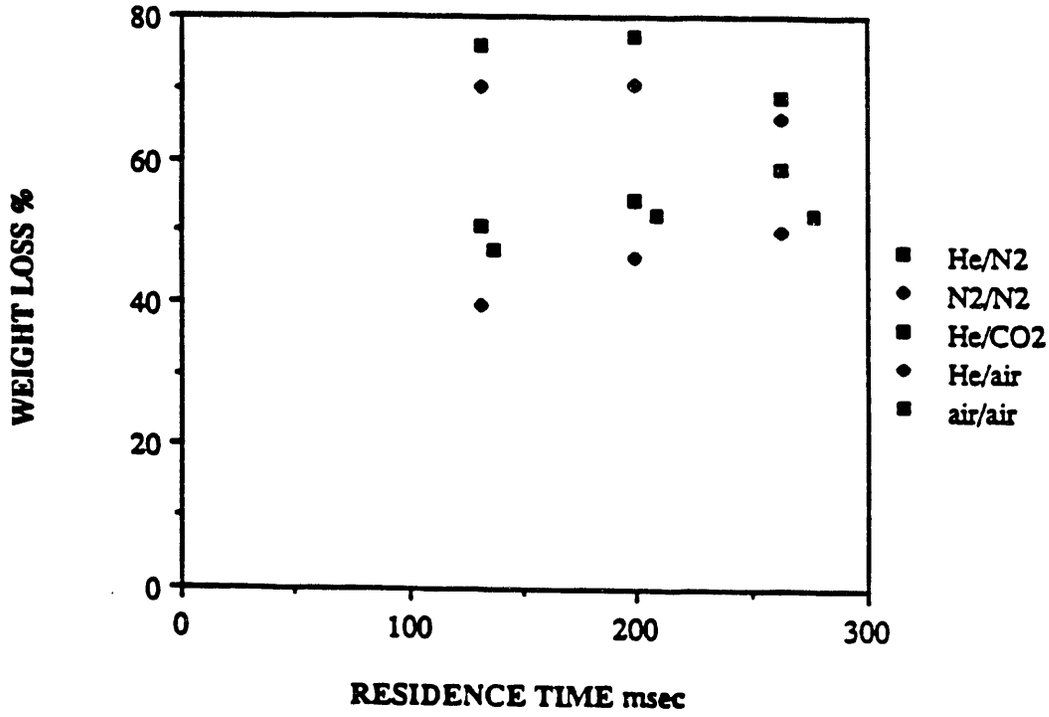

Effect of Reactor Atmosphere on Weight Loss for 81 μm Particles of PSOC-1451 at 1073 K

Figure 24

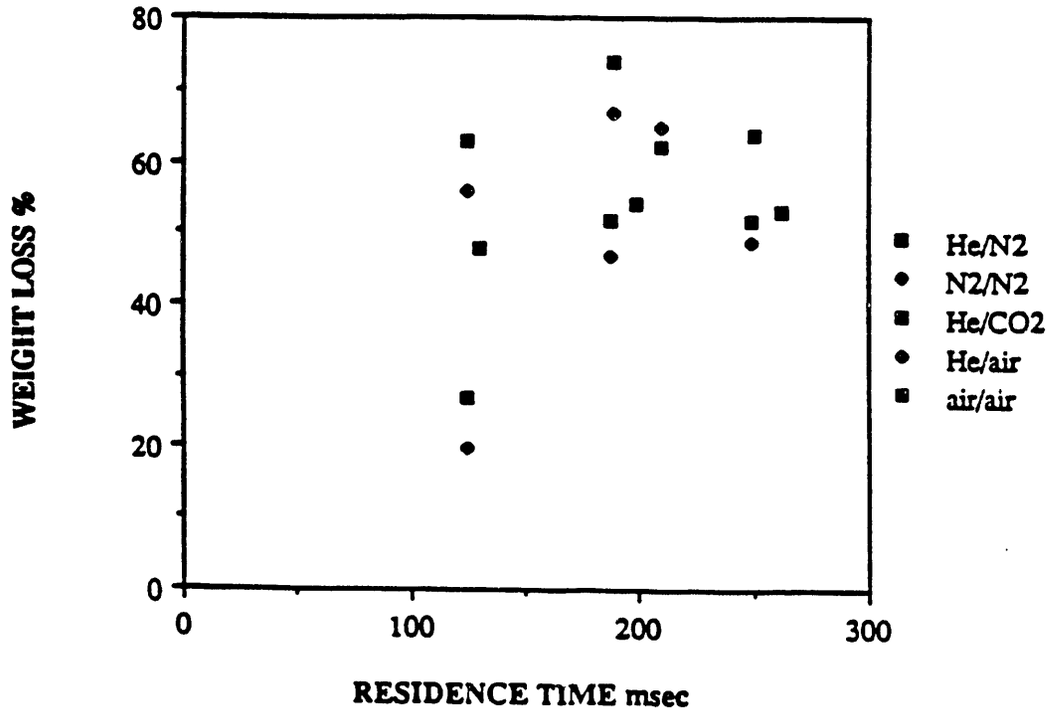

Effect of Reactor Atmosphere on Weight Loss for 115 μm Particles of PSOC-1451 at 1073 K

Figure 25

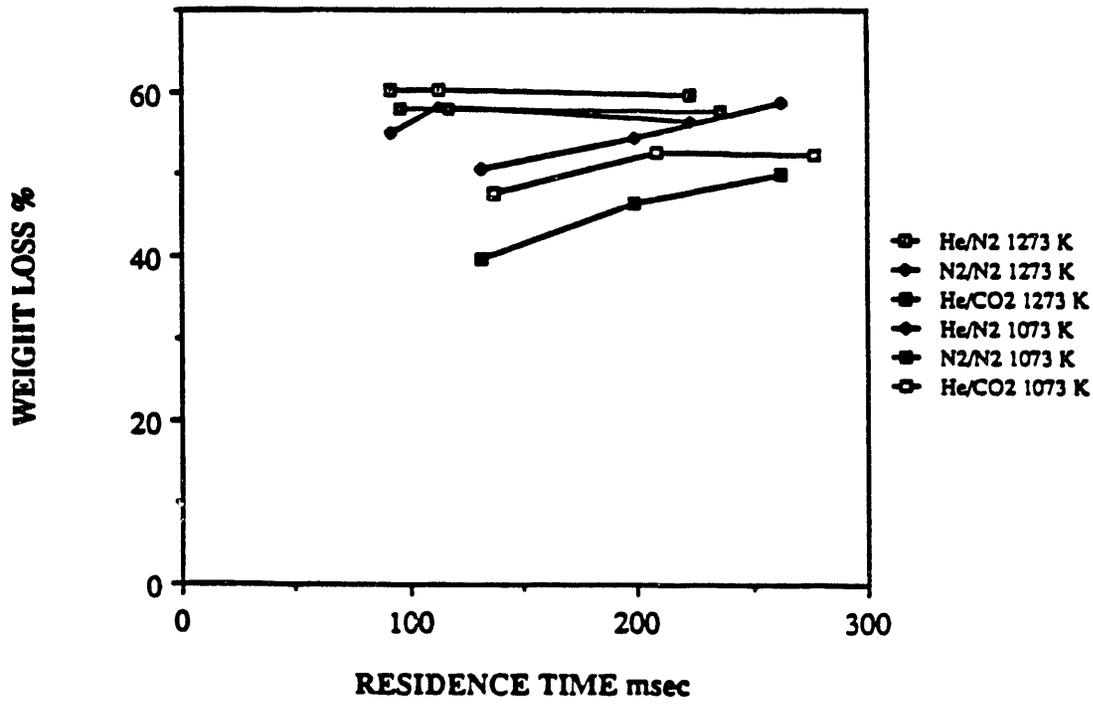

Effect of Temperature on Weight Loss for 81 μm Particles of PSOC-1451

Figure 26

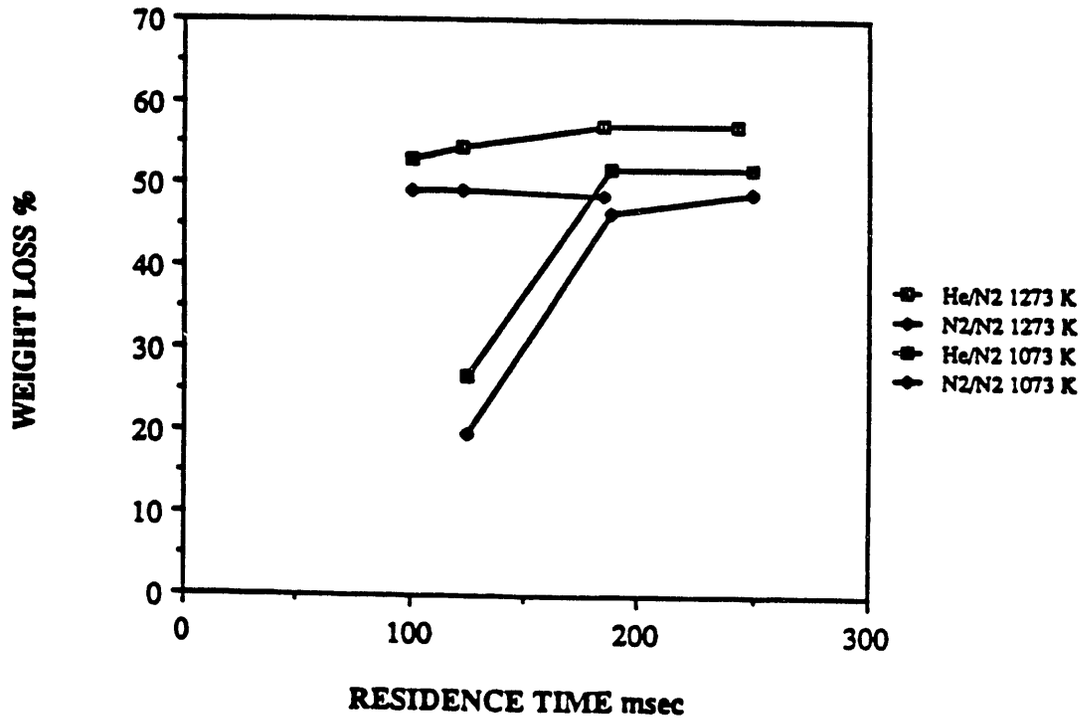

Effect of Temperature on Weight Loss for 115 μm Particles of PSOC-1451

Figure 27

COAL DEVOLATILIZATION / PYROLYSIS

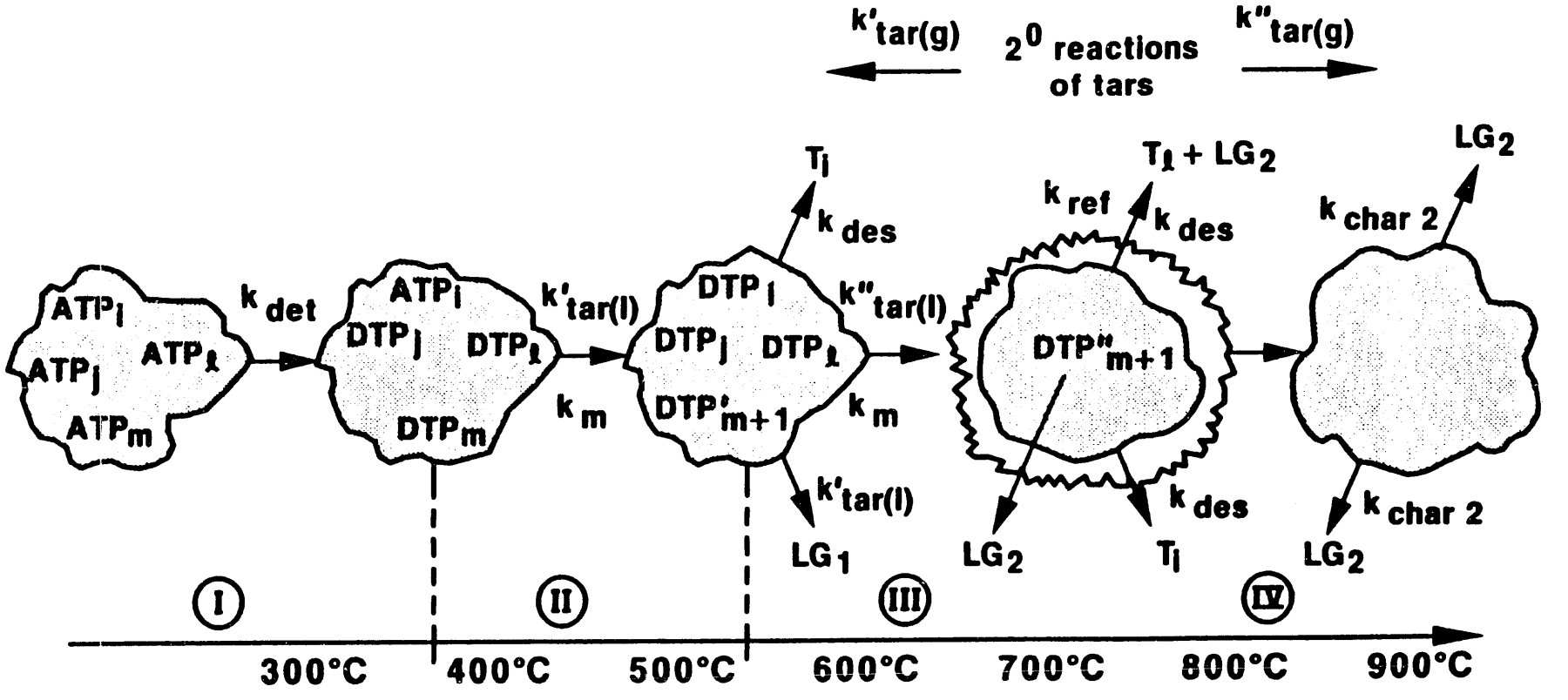

$k_{det} = k_{phy} + k_{chem}$

$k_{des} = k_{vap} + k_{conv} + k_{ned}$

RA2419TX.026

Figure 28

COAL DEVOLATILIZATION / PYROLYSIS

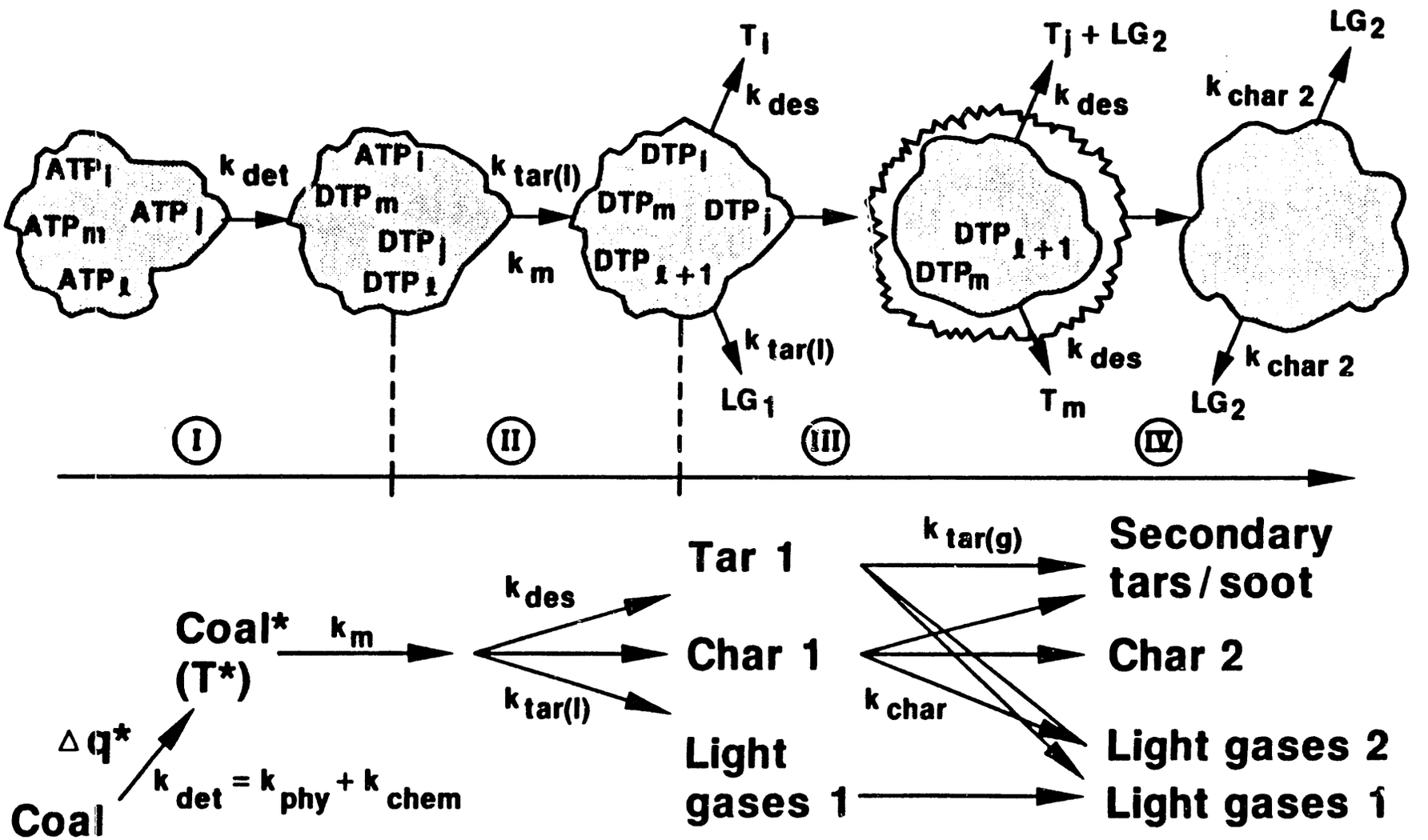

RA2418TX.027

Figure 29

PHASES OF DEVOLATILIZATION RELATIVE TO SIGMOID MASS LOSS CURVE

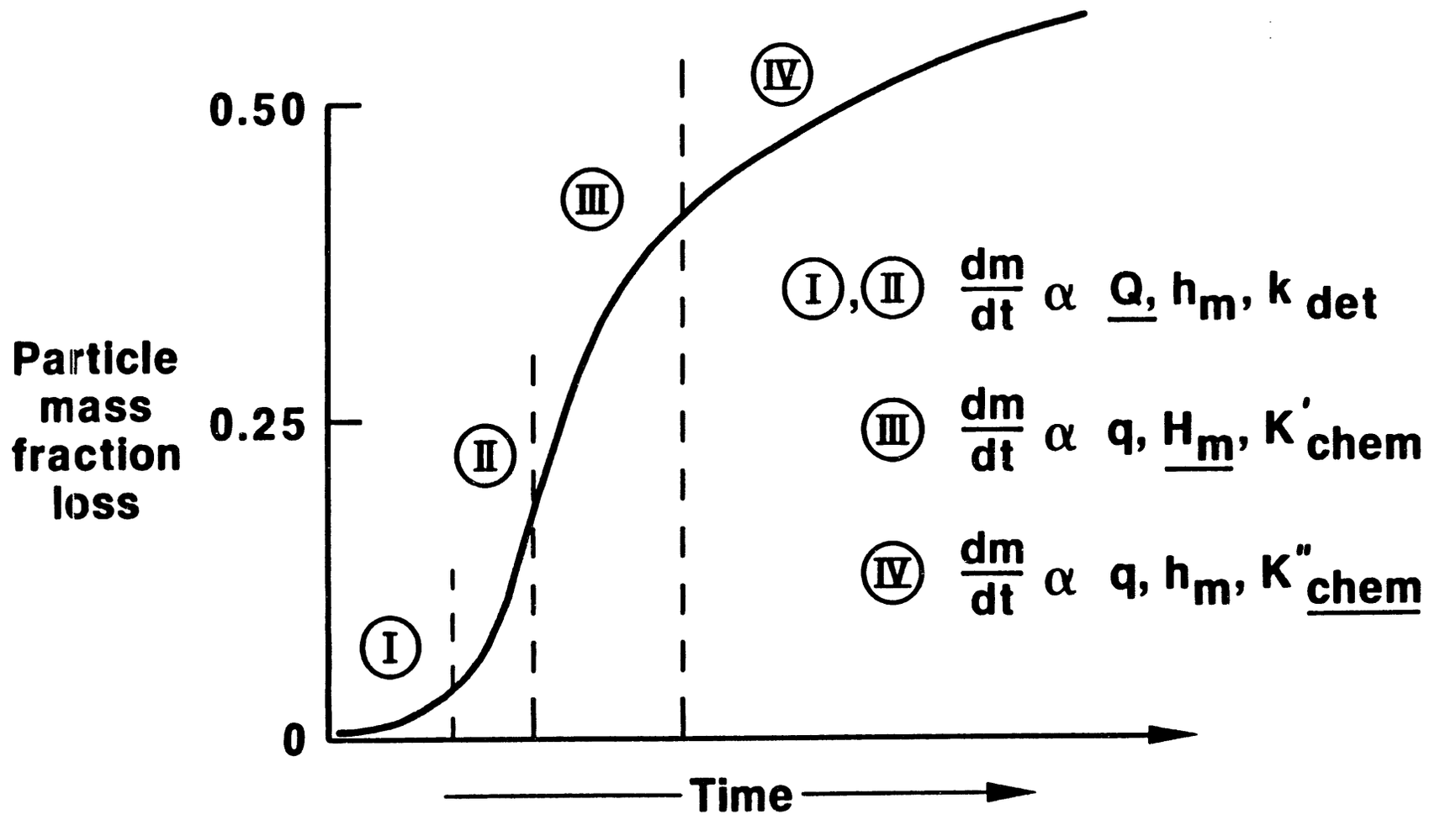

RA2415TX.004

Figure 30

TAR EVOLUTION RESPONSE vs. HEATING RATE INDEX

Index = net power density (300-600C)/particle size

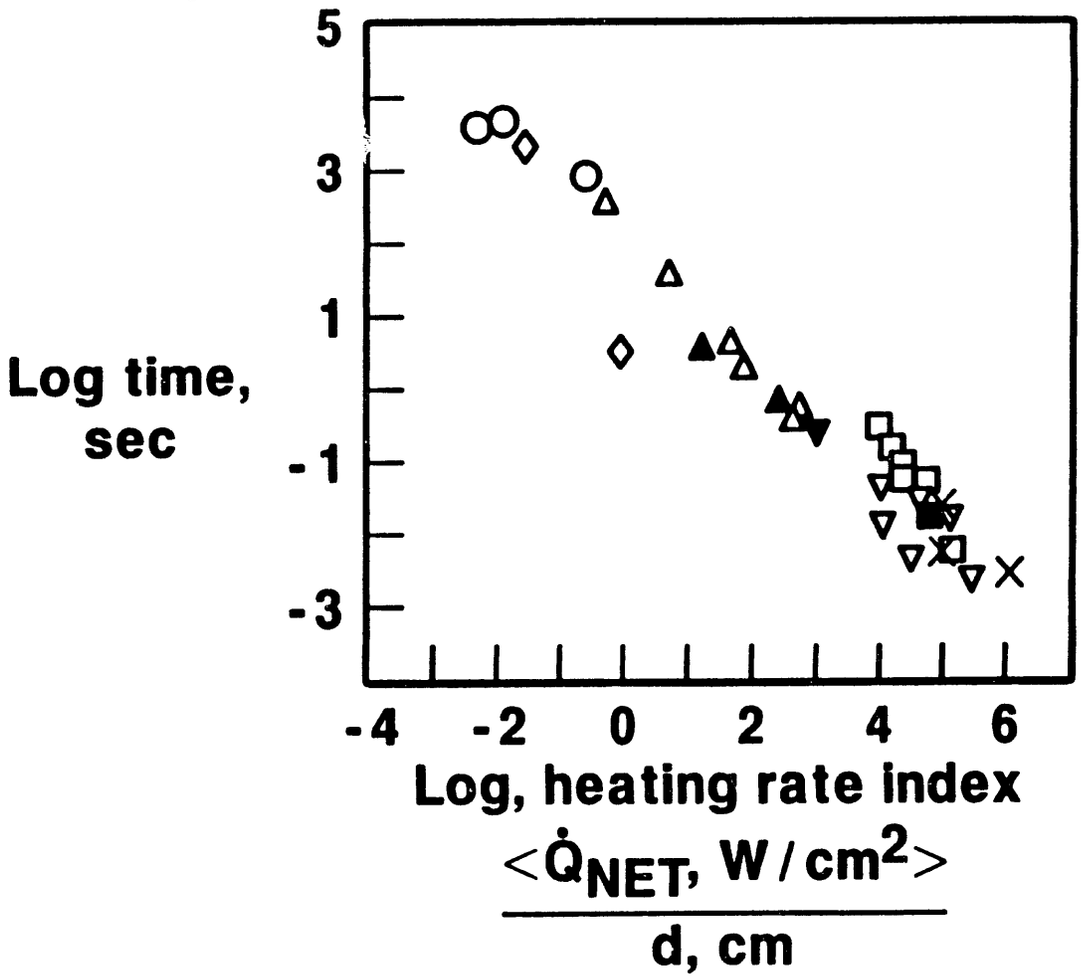

RA2415TX.018

END

DATE FILMED

11/14/91